Sea ice and productivity changes over the last glacial cycle in the Adélie Land region, East Antarctica, based on diatom assemblage variability

5   Lea Pesjak[1], Andrew McMinn[1], Zanna Chase[1], Helen Bostock[2,3]

[1]Institute for Marine and Antarctic Studies, University of Tasmania, Hobart, 7000, Australia
[2]University of Queensland, Brisbane, 4072, Australia
[3]National Institute of Water and Atmospheric Research (NIWA), Wellington, New Zealand

Correspondence to: Lea Pesjak (lea.pesjak@utas.edu.au)

Abstract

Although Ddiatoms can provide important paleoenvironmental information about seasonal sea ice extent, productivity, sea surface temperature and ocean circulation variability, yet there are still relatively few studies
15   analysing the last glacial cycle near the Antarctic continent. This study examines diatom assemblages over the last glacial cycle from core TAN1302-44, from offshore Adélie Land, East Antarctica. Four Two distinct diatom assemblages were identified using principal components analyses. The PC 1 assemblage is associated with the interglacial, sedimentary facies, Facies 1, and comprisesis characterized by *Thalassiosira lentiginosa, Actinocyclus actinochilus, Eucampia antarctica*, *Azpeitia tabularis* and *Asteromphalus hyalinus*, and is
20   associated with the interglacial, sedimentasedimentary ry facies, Facies 1, suggesting that the MIS 5e and Holocene interglacials time periods, were characterised by seasonal sea ice environments with similar ocean temperature and circulation. The PC 2 assemblage is associated with the glacial, Facies 2, and comprises is characterized by *Fragilariopsis obliquecostata, Asteromphalus parvulus, Rhizosolenia styliformis,* and *Thalassiosira tumida*, and is interpreted to reflect sea-ice environmentsis associated with the glacial, Facies 2.
25   The variability of PC2, *Chaetoceros dichaeta*, and a *Eucampia antarctica* terminal/intercalary ratio . This indicates that, during the MIS 4-2 glacial, and the last glaciation there was an increase in the length of the sea ice season compared with the interglacial period, yet still no permanent sea ice coveras indicated bythe dominance. The PC 2 assemblage is also associated with the glaciation and deglacial facies. There is anThe initial increase of PC 2 at the start of MIS 5d athe glaciation stage and then a gradual increase throughout late
30   MIS 4-2, suggests that sea ice cover steadily increased reaching a maximum at towards the end of MIS 2. The increase in sea ice during glaciation and MIS 4-2 glacial, is further supported by the increase in the *Eucampia* index (Terminal/Intercalary valve ratio) – an additional proxy for sea ice, which coincides with increases in PC 2. Furthermore, Aside from the statistical results, the visual the increase in the relative abundance of The PC 3 assemblage is associated with all four facies and comprises *Actinocyclus ingens, Actinocyclus actinochilus,*
35   *Thalassiosira oliverana* and *Fragilariopsis kerguelensis*, suggesting that reworking of sediments and an influx of older sediments occurred throughout the last glacial cycle. Finally, the PC 4 assemblage is associated with the deglacial, glaciation, and glacial facies and comprises *Fragilariopsis kerguelensis*, *Thalassiothrix antarctica*,

Chaetoceros bulbosum ~~and *Eucampia antarctica*,~~ at 40 cm and 270 cm, suggest~~ing~~s that during ~~the last glaciation,~~ the last two deglacials~~, and the early glacial,~~ there was a period of enhanced ~~upwelling of~~ nutrient

40 delivery ~~rich~~, ~~warmer water,~~ which is inferred to reflect an increase in upwelling of Circumpolar Deep Water. Interestingly, the diatom data suggest that during the last deglacial, the onset of increased Circumpolar Deep Water ~~during the last deglacial~~ occurred after the ~~rapid~~ loss of a prolonged sea ice season ~~at the end of last glacial~~ (decrease in PC 2), ~~and,~~but before the ice sheet started to retreat (increase in IRD). Together, these results suggest the changes in sea ice season potentially influenced the ocean's thermohaline circulation and ~~the~~

45 ~~changes in sea ice season~~ were important factors in driving the ~~during~~ climate transitions~~.~~. The results ~~fill a gap in~~contribute to our understanding of the sea ice extent and ocean circulation changes proximal to East Antarctica over the last glacial cycle and can be used to ground truth climate models.

1 Introduction

Ocean circulation near Antarctica's ice sheets is changing under the influence of climate change (Pri~~t~~chard et al. 2009; Depoorter et al. 2013; Alley et al. 2015; Silvano et al. 2018; Rignot et al. 2019; Minowa et al. 2021). T~~he~~two significant parameters in the atmosphere-ocean-ice sheet interaction system~~,~~ are duration and extent of seasonal sea ice and the ocean's thermohaline circulation. Antarctic sea ice is recognised as an important driver

55 of climate, as it affects the CO_2 exchange between the Southern Ocean~~,~~ and the atmosphere (Crosta et al. 2004; Kohfeld & Chase 2017), planetary albedo, and the ocean's thermal gradients (Gersonde & Zielinski 2000). Locally, its seasonal variation can affect ice shelves, increasing melting at the marine edge (Massom et al. 2018), ultimately destabilising the ice sheet (~~Prichard~~Pritchard et al. 2012). Furthermore, its seasonal expansion and retreat influences primary productivity; by limiting light ~~and lowering temperatures,~~ thus decreasing

60 productivity, although meltwater can also stimulate phytoplankton blooms (Knox 2006). The second significant parameter affecting climate is the ocean's thermohaline circulation. On the Antarctic margin this is driven by the formation of Antarctic Bottom Water (AABW), and the upwelling of Circumpolar Deep Water (CDW). Modern observations suggest that Antarctic ice sheet melt rates increase with enhanced upwelling of CDW (~~Prichard~~Pritchard et al. 2012; Rignot et al. 2019; Minowa et al. 2021) and ~~with~~this causes a decrease in the

65 production of AABW (Williams et al. 2016; Silvano et al. 2018), which may further influence ice sheet melt (Silvano et al. 2018). Understanding the past changes in sea ice and oceanography proximal to Antarctica, especially during past climate transitions and warmer than present interglacials, such as the last interglacial, MIS 5e, may provide further insight into the mechanisms of atmosphere-ocean-ice sheet interaction, to predict future changes and provide analogues for future outcomes under a warming climate (Masson-Delmotte et al. 2013).

70

Studies of diatom assemblages from ~~deep~~ ocean sediments can be used to reconstruct past ocean environments, including the extent and duration of seasonal sea ice, surface ocean circulation, and productivity (Cooke & Hays 1982; Pichon et al. 1992; Taylor & McMinn 2001; Crosta et al. 2004; Gersonde et al. 2005; Armand et al. 2005). Diatom studies are based on the identification and quantification of individual species and groups of

75 species, which are used to reconstruct paleoenvironments based on an understanding of the species' modern habitat (Table S1) from both water column (Medlin and Priddle 1990; Ligowski 1992; Moisan and Fryxell

1993) and from surface sediment studies (Zielinski and Gersonde 1997; Armand et al. 2005; Crosta et al. 2005). However, the interpretation can be influenced by processes such as selective dissolution within the water column and/ or sediment (Shemesh, Burckle & Froelich 1989; Zielinski & Gersonde 1997), winnowing of lighter species' valves by bottom currents (Taylor, McMinn & Franklin 1997; Post et al. 2014), or variable influx of terrigenous matter (Kellogg & Truesdale 1979; Schrader et al. 1993). Therefore, when reconstructing the past environment, it is important to consider all these processes.

There are many diatom-based studies of the interglacials, especially from the Holocene period from the Antarctic continental shelf (McMinn 2000; Taylor and McMinn 2001; Leventer et al. 2006; Crosta et al. 2007; Maddison, Pike & Dunbar 2012). However, advanced ice sheets, or permanent sea ice, in past glacials led to reduced, or no diatom productivity onover the Antarctic margincontinental shelf, and reduced productivity over the slope (Pudsey 1992; Lucchi 2002; Hartman et al. 2021). Additionally, advancing ice sheets would have removed most of the glacial sediment record from the continental shelves (Domack 1982; Escutia et al. 2003). This may be one of the reasons why there are so few studies from proximal Antarctica detailing the composition of diatom communities during glacial periods and over the last glacial to interglacial cycle (Caburlotto et al. 2010; Holder et al. 2020; Hartman et al. 2021; Li et al. 2021; Chadwick et al. 2022).

Overall, limited previous paleoenvironmental studies based on diatoms from the Antarctic continental slope suggest that, during the last glacial cycle. . During the last glacial, there was seasonal sea ice cover over the Adélie region (Caburlotto et al. 2010), a permanent sea ice cover in the Western Ross Sea (Tolotti et al. 2013), and a prolonged sea ice season in several regions including offshore Cape Adare, the Ross Sea (Hartman et al. 2021), offshore Enderby Land (Li et al. 2021) and offshore the Sabrina Coast (Holder et al. 2021). However, persistent biological productivity has been occasional glacial diatom blooms have been recorded from near offshore Cape Adare (based on diatom assemblagesstudies; Hartman et al. 2021), and the Weddell Sea (based on studies of foraminifera; Smith et al. 2010). These blooms have been suggested to represent localised polynyas (Arrigo & Van Dijken 2003) that existed during the last glacials. Only a couple of studies have looked into climate transitions during the last glacial cycle on the Antarctic margin. They show that during the last deglacial there was a decrease of the sea ice season and an increase in upwelling of CDW over the Enderby Land and Ross Sea continental margin (Li et al. 2021; Tolotti et al. 2013), while the last glaciation stage is reported to comprise oscillations in the sea ice season offshore Cape Adare (Hartman et al. 2021). Here we use diatom assemblages to understand the changes in the duration of the sea ice season and in CDW upwelling in the Adélie region over the last glacial cycle, ~140 ka, including the glaciation deglacial and deglacial glaciation transitions.

2 Materials and Methods

2.1 Site description

Core TAN1302-44 (Tan_44) was recovered using a gravity corer with a 2-tonne head, from the WEGA channel, on the continental slope north of Adélie Land and the George Vth Land coastline (Adélie region), at 64°54.75 S, 144°32.66 E, from 3,095 m depth (Fig. 1) by R/V Tangaroa in February 2013 during voyage TAN1302 (Williams 2013). The location is ~100 km north off the continental shelf break. The core site is located within the modern seasonal sea ice zone, (Fetterer et al. 2017), covered by sea ice from April to November each year (Fig. 1, Spreen, Kaleschke & Heygster 2008). The major oceanographic features of this region, which directly influence the site (Caburlotto et al. 2006; Williams et al. 2008), include Adélie Bottom Water (Adélie AABW), which forms below ~2,000 m from mixing of cooler Dense Shelf Water (DSW) formed on the shelf with warmer and nutrient rich CDW, and the wind-driven, westward flowing Antarctic Slope Front (ASF; Jacobs 1991; Williams et al. 2008; Fig. 1). The Antarctic Circumpolar Current (ACC), depicted in Fig 1. (Southern Boundary of the Antarctic Circumpolar Current front), does not influence the core site, but the ACC has a significant influence over Southern Ocean productivity and diatom species distribution (Supplement, Table S1).
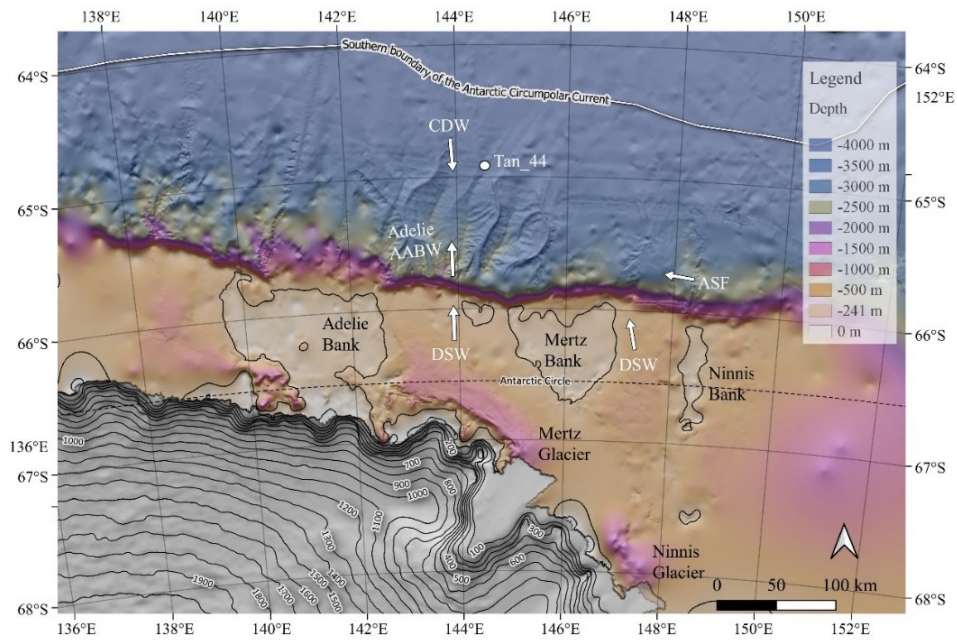
130

135
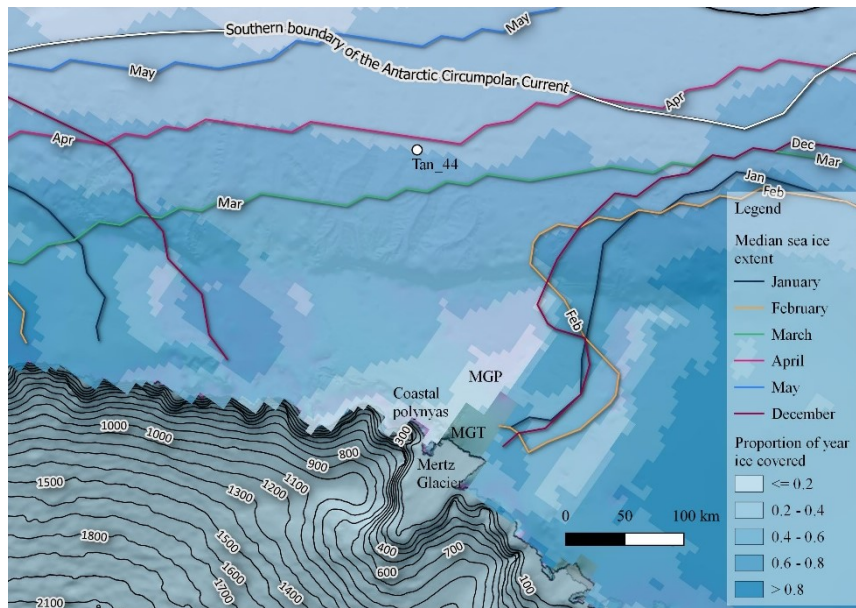
Figure 1 *Top*: location of core Tan_44 with respect to the regional bathymetry (Arndt et al. 2013); oceanography (Orsi et al. 1995; Williams et al. 2010) and cryosphere (Helm et al. 2014). The Mertz and Ninnis glaciers (Helm et al. 2014) are dominant glacial features in the region. Adélie and Mertz banks are prominent geomorphological features on the continental shelf, while deep channels are prominent on the continental slope. Tan_44 is located within the WEGA channel, on the continental slope. The site is influenced at present by Adélie sourced Antarctic Bottom Water (Adelie AABW), circumpolar deep water (CDW), and along slope flow of Antarctic Slope Front (ASF; Williams et al. 2010). *Bottom*: modern seasonal sea ice cover: the darkest blue showing regions covered by ice for more than 80% of the year, while the lightest blues indicates areas covered by ice less than 20% of the year (Spreen, Kaleschke & Heygster 2008), indicating the Mertz Glacier Polynya (MGP) and the coastal polynyas, where the main proportion of Adélie DSW forms, west of the Mertz Glacier Tongue (MGT; Williams et al. 2010). The figure also shows the core site is covered by sea ice from April to November each year (coloured lines; Fetterer et al. 2017).

2.2 Biogenic silica

~~Increased b~~Biogenic silica is used in this study as an indicator of ~~increased~~ paleoproductivity~~, and interglacials~~ (Bonn et al. 1998; Wilson et al. 2018). Analyses of biogenic silica were undertaken at 20 cm intervals down Tan_44. This study uses a modified wet-leaching technique (Mortlock and Froelich 1989; and DeMaster 1981), based on the premise that dissolution of fragile diatom tests is more rapid than the dissolution of silica from non-biogenic sources e.g. quartz grains. The time-series approach introduced by DeMaster (1981) was used. For quality control, two in-house standards were used from the Chilean and the Antarctic margin (Tooze et al. 2020). If the silica concentrations of the standards or the samples decreased with time during the hourly measurements, the whole experiment was repeated. The overall reproducibility of the method, assessed as the relative standard deviation of the standards, was +/-7%.

2.3 Si/Al (XRF)

Si/Al is used in this study as an indication of biogenic silica, and therefore paleoproductivity (Rothwell and Croudace 2015). X-ray fluorescence scanning (XRF) was completed at 2 mm resolution using an ITRAX

scanner (Gadd and Heijnis 2014) at the Australian Nuclear Science and Technology Organisation (ANSTO). The scanning was performed on u-channel sub-samples of the cores (of dimensions 2x2 cm, 1 m-long sections), which were stored in plastic containers and covered by thin plastic film. Anomalous spikes in data, identified by eye as significant increases or decreases occurring on mm-scale, were removed. The data was then smoothed using a 3-point running average.

2.4 Microfossil and micropyrite estimates

Microfossil and micropyrite estimates were completed using a binocular microscope, on a sievedthe sand (>63 µm) fraction, from samples collected every 20 cm down Tan_44.

2.4 Ice Rafted Debris (IRD)

Increased ice rafted debris (IRD) are used in this study as indicators of past Antarctic ice sheet retreat, and interglacial periods (Grobe et al. 1992; Cook et al. 2013; Patterson et al. 2014). IRD analysis was completed using two methods, counting visible grains from X-radiographs (grains ≥1 mm, in 5 cm sections), and counting sieved grains (> 500 µm-) per dry weight of total sample (grains >500 µm; and dividing the number by weight, g).. -The size >500 µm, medium sand (Patterson et al. 2014) was chosen as the size that defines IRD because laser particle diffraction of samples showed the grain size <250 µm forms the matrix of all the samples. This is in contrast to other Antarctic studies, which have defined IRD using a range of different sizes from >2 mm (Grobe et al. 1992; Diekmann et al. 2003), very coarse sand size, >1 mm (Lucchi et al. 2002; Pudsey & Camerlenghi 1998), >250 µm (Wilson et al. 2018), and >125 µm (Cook et al. 2013; Passchier 2011).

.

2.5 Radiocarbon datingFacies and age model

Radiocarbon dating was undertaken to support age model development, using the Acid Insoluble Organic Matter (AIOM) method, conducted at ANSTO, Sydney in April 2017 according to Hua et al. (2001); Fink et al. (2004); and Stuvier and Polach (1997). The raw radiocarbon ages were calibrated using CALIB, version 7.1, using the regional variation to the global marine reservoir correction, ΔR, of 830 yrs ±200 yrs, following previous work done in this region by Domack et al. (1989).

2.6 Facies model

A facies model was developed using the lithological unit characteristics (Supplement S1.2.1) and the combination of other data, primarily biogenic silica, Si/Al, and ice rafted debris (IRD). These data are described in the supplement (Fig. S1; Fig. The facies model comprises four facies which alternate down core and their overall facies characteristics are summarised results in Table 1along with the S2). . The definition of facies is interpreted to scopewas designed to capture large variability in physical and geochemical quality of sediment,

including large changes in productivity (biogenic silica, Si/Al and Ba/Ti) and sedimentology (IRD content; Wilson et al. 2018; Salabarnada et al. 2018; Wu et al. 2017; Bonn et al. 1998; Grobe & Mackensen 1992; Patterson et al. 2014).

2.7.1 Biogenic silica, Si/Al (XRF) and microfossil and micropyrite estimates

Biogenic silica varied from 0-22% (Fig. S1; Table 1; Fig. 2; Fig. 3). The highest values were found in the top 40 cm (10-22%), at 260-140 cm (12-16%), and at the base of the core at 540-520 cm (3-11%), coinciding with olive/grey sandy mud (Facies 1) and olive grey mud (Facies 1A). Moderate to low values (3-10%) occurred in olive mud (Facies 2A) and grey mud (Facies 2), with the exception of 18% at 140 cm within Facies 2 (Fig. S1; Fig. 3).

Si/Al (XRF) values varied from 14-28 (Fig. S1; Table 1; Fig. 2; Fig. 3). Higher values occurred within Facies 1, while lower values occurred within Facies 2.

Microfossil estimates were used to confirm productivity changes down core. This interpretation is dependent on the total amount of the sand fraction per sample and is therefore only an estimate of productivity. The estimates identified diatom and radiolaria species, where diatoms range from 0- ~20%, while the radiolaria range from 0- ~97%, per sand fraction of the sample (Fig. S1; Table 1). Intervals with highest diatom estimates (5-10%) are found in olive sandy mud (Facies 1). Intervals with highest radiolaria estimates (20-80%) coincide with 280-0 cm (Facies 1; 1A; 2; 2A), and 620-520 cm (Unit 1, 2A) sections. Pyrite coated foraminifera and radiolaria shells, and some framboidal pyrite are found at 80-60 cm (Unit 2A), and at 320-300 cm (Unit 2A; Fig. S1).

2.7.2 Ice Rafted Debris (IRD)

High counts of ice rafted debris (IRD; 4-36 grains/5 cm) are found in Facies 1 (Fig. S1; Table 1; Fig. 2; Fig. 3), with maximum counts found at 15-10 cm, at 255-250 cm and at 500-495 cm. Lower numbers of IRD (0-14 grains/5 cm) are found

2.6 Tan_44 Age Model

The age model of Tan_44 is based on the facies model and two radiocarbon dates from the top 25 cm of the core, using the premises . (Fig. 2; Table S2). The main characteristics of the faciessonably high sedimentation rate. Similar unreasonable C-14 dates at similar core depths, and even age reversals, were observed in cores

from the region (Pesjak 2022). The main characteristics of the facies (Table 1) suggest glacial to interglacial variability influenced the that variability in facies, including large changes in productivity proxies (biogenic silica, Si/Al and Ba/Ti) and IRD content present glacial to interglacial climate variability; (-Wilson et al. 2018; Salabarnada et al. 2018; Wu et al. 2017; Bonn et al. 1998; Grobe & Mackensen 1992;) and IRD (Patterson et al. 2014). ; Fig. S1 2), which show a strong coincidence with the global benthic δ¹⁸O stack (Lisiecki & Raymo 2005). The radiocarbon dates (Fig. 2) indicate the top of the core was deposited between 16.2–5.2 ka, suggesting Facies 1 is of Holocene and Facies 2A of Late Pleistocene age. The interpretation of Facies 1 at 270–230cm being the last interglacial, MIS5e. and not an earlier interglacial is strengthened by the fact that we did not observe any *Rouxia leventerae* (last occurrence at MIS6–5e boundary) in any samples examined.

Table 2.7 Radiocarbon dating (AIOM) conventional and calibrated results.

facies model and Si/Al for core Tan_44. The age model is based the facies model and supported by radiocarbon dating of two depths at the top of the core, and the comparison of Si/Al to the global benthic stable isotopes stack LR04 (Lisiecki and Raymo, 2004).

2.6 Diatom counts and Shannon Wiener biodiversity index

Diatoms Diatom assemblages species were counted from or samples taken every 10 cm down core Tan_44 (starting at 5 cm, then 20 cm). The samples were processed following the methods outlined in Taylor & McMinn (2001). A small section of the sediment core (<0.5 cm thick) was soaked in 15% hydrogen peroxide overnight, to remove organic matter and to disaggregate any clay. The samples were rinsed with deionised water through a 100 µm and a 10 µm sieve, in order to obtain a >10 µm, <100 µm grain fraction. This fraction was left overnight to settle. Excess water above the sample was pipetted out, and the remaining sample was stored in a 100 ml tube. A drop from each shaken tube was pipetted onto a glass cover slip over a hotplate at 50°C, to evaporate excess water. The samples were then mounted with Norland Optical Adhesive 61 and cured in sunlight. Diatom identification and counts were undertaken using a Nikon light microscope (Eclipse Ci, DS-Ri2) at 1000 X magnification. Each sample was traversed until >400 valves were counted. Broken valves that were >50% complete were included in the count and in the case of elongated species, such as *Thalassiothrix* and *Trichotoxon* that are subject to fragmentation, only the ends were counted (McMinn et al. 2001). Lower valve numbers, of less than 400 valves per slide, were encountered in samples at 80 cm, and from 350-300 cm. The numbers of valves within the 350-320 cm samples were extremely low (7-16 valves per slide).

Figure 2 Diatom counts, facies model and Si/Al for core Tan_44. The age model is based the facies model and supported by radiocarbon dating and comparison of Si/Al to the global benthic stable isotopes stack LR04

(Lisiecki and Raymo, 2004). ~~The age of facies contacts are derived from the marine isotope stage boundaries (Lisiecki and Raymo 2004).~~

275 Due to the scarcity of valves in these samples, and well below 400 valves per slide observed within 320-300 cm, only samples from 290-5 cm are included in statistical analysis. ~~The number of diatom valves on a whole slide is considered a qualitative measure of diatom abundance.~~

Some species were grouped together due to morphology and habitat indicators, these groups are the
280 *Fragilariopsis* group, comprising *F. obliquecostata, F. sublinearis, F. cylindrus*, and *F. rhombica*; the *Thalassiothrix* group, comprising *Thalassiothrix antarctica, Thalassiothrix longissima* and *Trichotoxon reinboldii, and the Rhizosolenia* group, comprising *Rhizosolenia styliformis, Rhizosolenia (twin process) antennata, R. antennata, R. hebetata, R.setigera, R. polydactyla, Rhizosolenia sp.,* and *Proboscia intermis.*

285 The relative abundance of each species (or group) was expressed as the number of valves of that species divided by the total valve count (expressed as %). Species ~~or species groups with <2% in at least one sample were excluded from the distribution description, and species~~ with >~~2~~1.8% in at least two samples were ~~excluded from~~included in statistical analysis~~.~~, ~~The,~~except~~ion in both cases, was inclusion of lower abundance species~~ in case~~ss where species were grouped together, due to similarity in habitat indicators (i.e.,~~of the *Fragilariopsis*
290 ~~(sea ice species)~~ group, which apart from *Fragilariopsis obliquecostata* (present at >1.8% in at least 2 samples) also included much rarer sea ice species (*F. sublinearis, F. linearis, F. cylindrus* and *F. rhombica).*

Species or species groups present at >1.8% in at least 1 sample, and thus excluded from statistics, were included in results and discussion due to their environmental indications (Table S1). These species include the ~~species~~
295 ~~groups,~~*Thalassiothrix antarctica* group, represented mainly by ~~) or morphology (i.e.,~~*Thalassiothrix antarctica,* ~~and *Trichotoxon*~~, and the *Rhizosolenia* species group, presented mainly by *Rhizosolenia styliformis* and *Rhizosolenia* (twin process) *antennata* (the sum of both species was up to 1.2-1.6% in three samples). The *Thalassiothrix* group is also discussed where there is a significant increase in broken valves, yet the relative abundance (i.e., counted valve ends) is 0%.~~, and *Rhizosolenia* group (*Rhizosolenia styliformis* and *Rhizosolenia*~~
300 ~~antennata). where~~ in ~~which case the representative species of a group needed to be >2% in at least one sample but members of the group only required >1~~at least 2 ~~valve per sample to be included in a group.~~.

The *Eucampia* index~~,~~ was also ~~used aside from main, statistical analysis,~~ as an indicator of ~~increased~~ sea ice presence (Fryxell et al. 1991). It represents the ratio of the number of t~~T~~erminal valves to the number of i~~over~~
305 ~~I~~ntercalary valves ~~of ratio of~~*Eucampia antarctica* species, and its increase is associated with more sea ice in the environment. In the open ocean the *Eucampia antarctica* species grow in longer chains, while in sea ice waters~~,~~ they grow in shorter chains (Fryxell 1991). The chains comprise intercalary valves in the middle, and terminal valves at the ends, and therefore, the more terminal valves, the more sea ice (Fryxell 1991: Kaczmarska et al.

1993). The *Eucampia* index was only ~~considered from statistically reliable samples,~~calculated where the total *Eucampia antarctica* count was 100 valves and above.

An assessment of the diversity of diatoms in each sample was determined using the Shannon-Wiener diversity index. The Shannon-Wiener diversity index (Spellerberg et al. 2003) was calculated according to the formula:

$$H = -\sum_{i=1}^{n} [p_i \: x \ln p_i]$$

2.~~8~~7 Statistical analyses: cluster analysis and principal component analysis

The relative diatom abundance data set was analysed using a hierarchical cluster analysis and principal component analysis (PCA), in Statistical Package for Social Sciences (SPSS) software package. For these analyses the relative abundance data was logarithmically transformed using the equation: Abundance = $\log_{10}$ (x+1), where x= relative abundance (%), (Taylor, McMinn & Franklin 1997). Cluster analysis (Burckle 1984; Truesdale & Kellogg 1979) involved calculating the average distance between groups. The PCA (Taylor, McMinn & Franklin 1997; Zielinski & Gersonde 1997) was undertaken in two stages. In Q-mode, investigating relationships between variables (species), and in R-mode, analysing relationships between samples (Shi 1993). The factor variance used to extract the number of components for Q-mode analysis was established at ~~>>10~~ ~~9~~12 % variance. The factor variance used to extract the number of components for R-mode analysis was established at ~~>>0.4~~ ~~5~~42 %. Factor variance is the amount of the total variance of all of the variables accounted for by each component (factor) (https://www.ibm.com/docs/en/spss-statistics). Outputs from both Q and R analyses underwent a Varimax rotation. Rotation maintains the cumulative percentage of variation explained by the chosen components ~~(in this case >8% and >1.4%)~~, but the variation is spread more evenly over the components (https://www.ibm.com/docs/en/spss-statistics). Finally, to demonstrate the strength of the correlation between the components and productivity proxies (Si/Al and biogenic silica), ~~regression~~ bivariate Pearson Correlation analyses were undertaken using SPSS.

3 Results

3.1 Biogenic silica, Si/Al ~~(XRF)~~, ice rafted debris ~~(IRD)~~, and the facies model

The facies model is comprised of four facies which alternate down core (Supplement Fig. S1; Table 1). The main parameters determining the facies (biogenic silica, Si/Al and IRD) are described below, The interpretation of the facies is further described in the Age Model section.

Biogenic silica varied from 0-22% (Fig. S1; Table 1; Fig. 2; Fig. 3). The highest values were found in the top 40 cm (10-22%), at 260-140 cm (12-16%), and at the base of the core at 540-520 cm (3-11%), coinciding with olive/grey sandy mud (Facies 1) and olive grey mud (Facies 1A). Moderate to low values (3-10%) occurred in olive mud (Facies 2A) and grey mud (Facies 2), with the exception of 18% at 140 cm within Facies 2 (Fig. S1; Fig. 3).

Si/Al (XRF) values varied from 14-28 (Fig. S1; Fig. S2; Table 1; Fig. 2; Fig. 3). Higher values occurred within olive/ grey sandy mud (Facies 1), while lower values occurred within olive mud (Facies 2A), olive grey mud (Facies 1A), and grey mud (Facies 2).

High counts of ice rafted debris (IRD; 4-36 grains/5 cm) are found in olive/ grey sandy mud (Facies 1; (Fig. S1; Table 1; Fig. 2; Fig. 3), with maximum counts found at 15-10 cm, at 255-250 cm and at 500-495 cm. Lower numbers of IRD (0-14 grains/5 cm) are found in grey mud (Facies 2), olive grey mud (Facies 2A) and olive mud (-Facies 1A).

Table 1 Summary of the characteristics of the four facies present in core Tan_44.

CHARACTERISTICS:	FACIES:			
	1) OLIVE SANDY MUD	2A) OLIVE MUD	2) GREY MUD	1A) OLIVE GREY MUD
Colour	Olive; grey (base layer)	Olive	Grey	Olive grey
Structure	Massive; bioturbation; rare laminae	Massive; bioturbation;	Massive; bioturbation; laminae; traction structures	Massive; bioturbation;
IRD (grains/5 cm)	0-36	0-10	0-14	1-15
IRD (grains/g)	2-15	0-1	0-1	0-2
% Vf-f sand	1-19	1-7	0-5	0-6
% Vc silt	8-27	3-18	4-13	7-17
Zr/Rb	0.6-2.3	0.5-1.9	0.4-1.4	0.7-1.4
% Biogenic silica	3-22	4-10	3-18	10-11
Si/Al	15-28	14-23	12-20	16-21
Ba/Ti	0.01-0.06	0-0.06	0-0.04	0.03-0.05
INTERPRETATION:	Interglacial	Deglacial	Glacial	Glaciation

3.2 The Radiocarbon dates, and the age model

The two top radiocarbon dates (Fig. 2) indicate the top of the core was deposited between 16.2- 5.2 ka, suggesting Facies 1 is of Holocene and Facies 2A of Late Pleistocene age. Facies 1 at 270-230cm is interpreted as being the last interglacial, MIS5e, supported by the fact that we did not observe any *Rouxia leventerae* (last occurrence at MIS6–5e boundary; (Zielinski and Gersonde 2002) at these depths. The ~~two top radiocarbon dates suggest~~ two deeper radiocarbon dates (Table 2) were not included in the interpretation because they imply an unreasonably high sedimentation rate. Similar unreasonable C-14 dates at similar core depths, and even age reversals, were observed in other cores from the region (Pesjak 2022).

The main characteristics of the facies found in Tan_44 (Table 1) in combination with the radiocarbon dates ~~of~~ at the top of core, ~~(Table 1)~~ suggest glacial to interglacial variability influenced the productivity proxies (biogenic silica, Si/Al and Ba/Ti; Wilson et al. 2018; Salabarnada et al. 2018; Wu et al. 2017; Bonn et al. 1998; Grobe & Mackensen 1992) and IRD (Patterson et al. 2014; Fig. S1; Fig. 2), which show a strong coincidence with the global benthic $\delta^{18}O$ stack (Lisiecki & Raymo 2005).

Table 2 Radiocarbon dating (AIOM) conventional and calibrated results.

Lab No.	Sample	Depth (cm)	Conventional radiocarbon age (yr BP)	Error ± (yr)	δ 13C	Calibrated age (cal. yr BP); ΔR=830+/-200	Calibrated mean (yr BP)
OZV390	Tan44_0cm	0.5-3.5	5,765	45	-25	4,971-5,478	5,233
OZV391	Tan44_25cm	25.5-26.5	14,660	80	-23.6	15,837-16,468	16,160
OZV392	Tan44_35cm	35.5-36.5	18,470	90	-23.9	20,504-21,082	20,803
OZV393	Tan44_45cm	45.0-46.0	19,150	140	-25	21,340 - 22,007	21,682

.
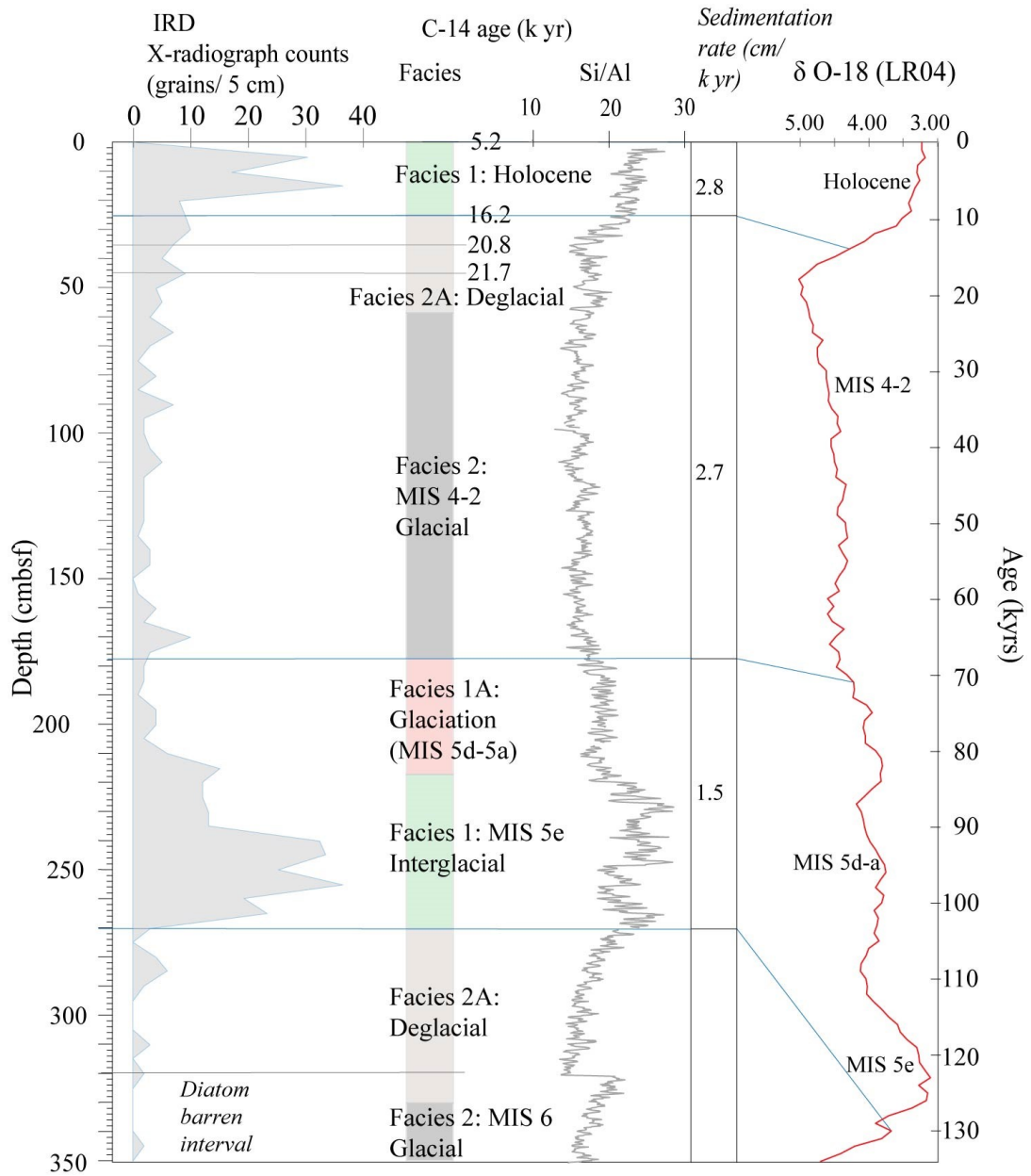
Figure 2 IRD counts, facies model and Si/Al for core Tan_44. The age model is based the facies model and supported by radiocarbon dating of two depths at the top of the core, and the comparison of Si/Al to the global benthic stable isotopes stack LR04 (Lisiecki and Raymo, 2004).

390

395   **3.3**3.2 **Species distribution, biodiversity, and abundance**

All samples contained well-preserved diatom assemblages with little evidence of dissolution, such as frustule thinning. Of the 53 species identified in 34 samples (Table S5S4), 24 species (Table S1) were included in the species distribution description and of those, 12 species were included in statistical analysis (12 species andwith an additional 4 more addedincluded from the *Fragilariopsis* group; Fig. 3). One extinct species. *Actinocyclus ingens* (Cody et al. 2008) was found at 11% at 60 cm, and at 3% at 280 cm at the glacial to deglacial facies boundaries MIS 2/1 and MIS 6/5e. Relatively high Shannon Wiener index values were relatively highof (-1.6 - 2) were found at 40 cm and at 220-130 cm, within the glaciation and glacial (MIS 4-2) facies (Fig. 3). The interval from 350-320 cm is considered barren (Fig. 3), it contains only a few specimens of robust valve forms such as *Thalassiosira lentiginosa*, *Eucampia antarctica* and *Actinocyclus actinochilus* (Table S4). This interval also contains pyritised shells, which were also found at 80-60 cm, during the Last Glacial Maximum (Fig. S1). The distribution of species (between 290-5 cm depth) is described below, in the order of species habitats (Table S1).

The most abundant species was *Thalassiosira lentiginosa* (Fig. 3), which comprised >20% of the total throughout the core and >55% of the total from 50-5 cm and 270-230 cm, coinciding with the interglacial and deglacial facies, respectively. The minimum abundances for this species were between 170-60 cm, coinciding with the glacial facies (Fig. 3). The second most abundant species was *Eucampia antarctica* (Fig. 3). It had maximum abundances of 18-62%, occurring in the 210-60 cm interval (glacial and glaciation facies) and within the 290-280 cm sample (glacial and deglacial facies). Relatively high *Eucampia* abundances, >30%, were found at 140-110 cm, at 210 cm, and 290-280 cm, while exceptionally high values (59-62%) occurred within 100-70 cm. The lowest abundances of *Eucampia antarctica* were found in the 50-5 cm interval (2-8%), and 270-220 cm (2.7-18%), both within interglacial and deglacial facies. below

The following section describes species that comprised 25% or less relative abundance (Fig. 3). *Fragilariopsis kerguelensis* was the third most abundant species, with maximum values (17-25%) found at 220-210 cm and 50-40 cm, within the glaciation/interglacial and deglacial facies, respectively. These are also the intervals where both the *Thalassiosira lentiginosa* and *Eucampia antarctica* numbers decreased. High abundances of *Actinocyclus actinochilus* (7-13%) occurred at 140-50 cm and 290-280 cm (glacial and deglacial facies), while lower values (4-7%) were found at 240-150 cm (glacial, interglacial and glaciation facies) and low values (1.6-4%) at 40-5 cm (interglacial, deglacial). *Actinocyclus ingens* was found at 60 cm (at 11% abundance) and at 280 cm (at 3% abundance), within two different glacial to deglacial facies boundaries. The *Fragilariopsis* group, which was mostly comprised of *F. obliquecostata* with lower abundances of *F.*

The most abundant species in the samples were those associated with open ocean environments, *Thalassiosira lentiginosa* (20-73% of the total counts); *Eucampia antarctica* (2-62 %), and *Fragilariopsis kerguelensis* (1-25%; Fig. 3). The highest abundance of *Thalassiosira lentiginosa* (>55%) occurred at 50-5 cm (interglacial and deglacial facies), at 150 cm (glaciation) and 270-230 cm (interglacial). Highest abundance of *Eucampia antarctica* (18-62%); occurred at 210-60 cm (glacial and glaciation), at 290-280 cm (deglacial), and at 250 cm (interglacial). Maximum *Fragilariopsis kerguelensis* (17-25%) was found at 220-210 cm (glaciation) and at 50-40 cm (deglacial). Less abundant open ocean species (Fig. 3) wereincluded: *Thalassiosira. oliveriana* (highest

435 abundance of 4-8%) at 20-5 cm, 60 cm, 200-190 cm, 240-230 cm, and at 280 cm, within interglacial, deglacial and glacial facies; *Azpeitia tabularis* ~~(highest~~*sublinearis, F. linearis, F. cylindrus* and *F. angulata,* attained maximum abundances of 8% at 160-200 cm, within the glacial facies. *Thalassiosira oliverana* and *Thalassiosira tumida* ranged in abundance between 0 8% and 0 4%, respectively. Maximum *T. oliverana* abundances were at 20-5 cm, 50 cm, 210-190 cm, 240-230 cm, and at 280 cm within the interglacial, deglacial and glacial facies.~~

440 ~~Maximum *T. tumida* abundances were at 240-220 cm and 190-160 cm, within interglacial and glacial facies.~~

 ~~The following species occurred at a maximum~~ with abundance of ~~4% in~~3-6%~~)~~ at ~~least one sample. *Chaetoceros dichaeta,* was found~~50-5 cm, and ~~at 200~~260-250 cm, within the ~~the glaciation facies~~interglacial and deglacial facies; *Chaetoceros bulbosum*~~, found~~ ~~(with 4%),~~ at 40 cm, within the deglacial facies; *Chaetoceros dichaeta*

445 with ~~(4%),~~ at 200 cm, within the glaciation facies; *Rhizosolenia* ~~group, which is dominated by *Rhizosolenia styliformis,* and contains lower abundances of *Rhizosolenia antennata* (twin process), is found at 80 cm, 140~~*Asteromphalus hyalinus* with ~~(2-3%),~~ at 150 cm, and ~~200-160~~250 cm~~, all~~ within the glacial facies~~ facies;~~ ~~the. :~~*Thalassiothrix* group, dominated by *Thalassiothrix antarctica* ~~(while,~~ ~~, with lesser occurrence of *Thalassiothrix longisima*longissima and *Trichotoxon*Trixotoxon *reinboldii* are sparce) was found at 40 cm and~~

450 ~~260 cm, within the deglacial and interglacial facies, but as mentioned above, the abundance may be underestimated as samples at 40 cm and 270 cm (deglacial intervals)~~ had a relative abundance of ~~(3%)~~ at 40 cm (Fig. 3), and a high ~~amount~~ ~~visual abundances of~~abundance ~~comprising~~of broken *Thalassiothrix* valves ~~(which were~~ ~~,~~relative to other samples, at 40 cm, and 270 cm (Fig. 5), although the 270 cm sample had 0% relative abundance (i.e., valve ends counted). ~~,b~~Both intervals occur within the deglacial facies~~)~~~~.~~: *Thalassiosira oestrupii*

455 ~~had higher abundances~~(with 2-3%), at 50-30 cm (deglacial)~~,~~ ~~140-130 cm~~ and ~~at~~ 240 cm~~, within the deglacial, glacial and~~ (interglacial)~~ facies, respectively~~; *Asteromphalus parvulus* ~~was found at 180-160 cm,~~ with ~~(~~1.8% at 170 cm, and 2%~~),~~ at 200 cm, within the glacial facies; and the *Rhizosolenia* group, dominated by *Rhizosolenia styliformis,* and less *Rhizosolenia* (twin process) *antennata*~~(~~, with relative abundance of ~~(~~1.8-1.9~~2~~%~~),~~ at 140 cm, 170 cm, and at 200 cm~~and at 240-230 cm~~, within the glacial facies.

460

 Open ocean - sea ice edge species (Table S1) comprised *Actinocyclus actinochilus* found from 7-13%, at 140-50 cm and 290-280 cm, within ~~the~~ glacial and ~~interglacial~~deglacial facies~~, respectively; and *Asteromphalus hyalinus*; while~~and *Thalassiosira* ~~, was found~~*tumida,* found from 2-4% at 170-~~150~~160 cm, ~~at 240~~200-190 cm, within the glacial, and ~~at 270~~250-230 cm, within ~~the glacial,~~the interglacial~~ and deglacial~~ facies.

465

 Sea ice proxies (Table S1) ~~were~~comprised the *Fragilariopsis* group species, *Eucampia* index and *Stellarima microtrias.* The *Fragilariopsis* group comprised a dominant species *Fragilariopsis obliquecostata* and much lower abundances of *F. sublinearis, F. linearis, F. cylindrus* and *F.* ~~Eucampia antarctica terminal/ intercalary ratios were~~rhombica. *Fragilariopsis obliquecostata* is a species that lives in sea ice (Crosta et al. 2022; Garrison and Buck 1989; Armand et al. 2005). The *Fragilariopsis* group attained maximum abundances from 5-8% at

470 160-200 cm, within the glacial facies. The *Eucampia* index is elevated between 140-60 cm within the late MIS 4-2 glacial facies. The *Eucampia* index is not considered at intervals within 50-5 cm, and 270-220 cm, and at

depths of 150 cm, 180 cm, and at 200 cm (Fig. 3), due to *Eucampia antarctica* counts being <100 valves per sample, considered too low to be statistically reliable. highest (0.4-0.8) at 140-20 cm, in the glacial, deglacial and interglacial facies; an unusually high ratio of 1.4 occurred at 50 cm in the deglacial facies (Fig. 3). However, this high value is coincident with sea ice species indicators, such as *Fragilariopsis* species. This value may be unreliable due to the very low abundance of *Eucampia antarctica* too(2%)reliably use thetoo low to use the index,order to consider the data statistically correct for calculating the index within these intervals. Consistently high values of the ratio (0.4-0.8) together with high counts of *Eucampia antarctica* valves in general, were found within 140-60 cm, coincident with upper MIS 4-2 glacial (Fig. 3). Relatively high values (0.4) of the ratio were also found in the glaciation facies. Relatively low values (0-0.3) of the ratio were found in the lower glacial (MIS 4-2) interval. *Stellarima microtrias* was found >2% only at 270 cm, within the deglacial.

MIS 2/1 and MIS 6/5e

The interval from 350-320 cm is considered barren (Fig. 3), that is, it contains only a few specimens of robust valve forms such as *Thalassiosira lentiginosa*, *Eucampia antarctica* and *Actinocyclus actinochilus* (Table S5), which could have been reworked. This interval also contains pyritised shells, which are also found at 80-60 and at 320-300 cm (Fig. S1).
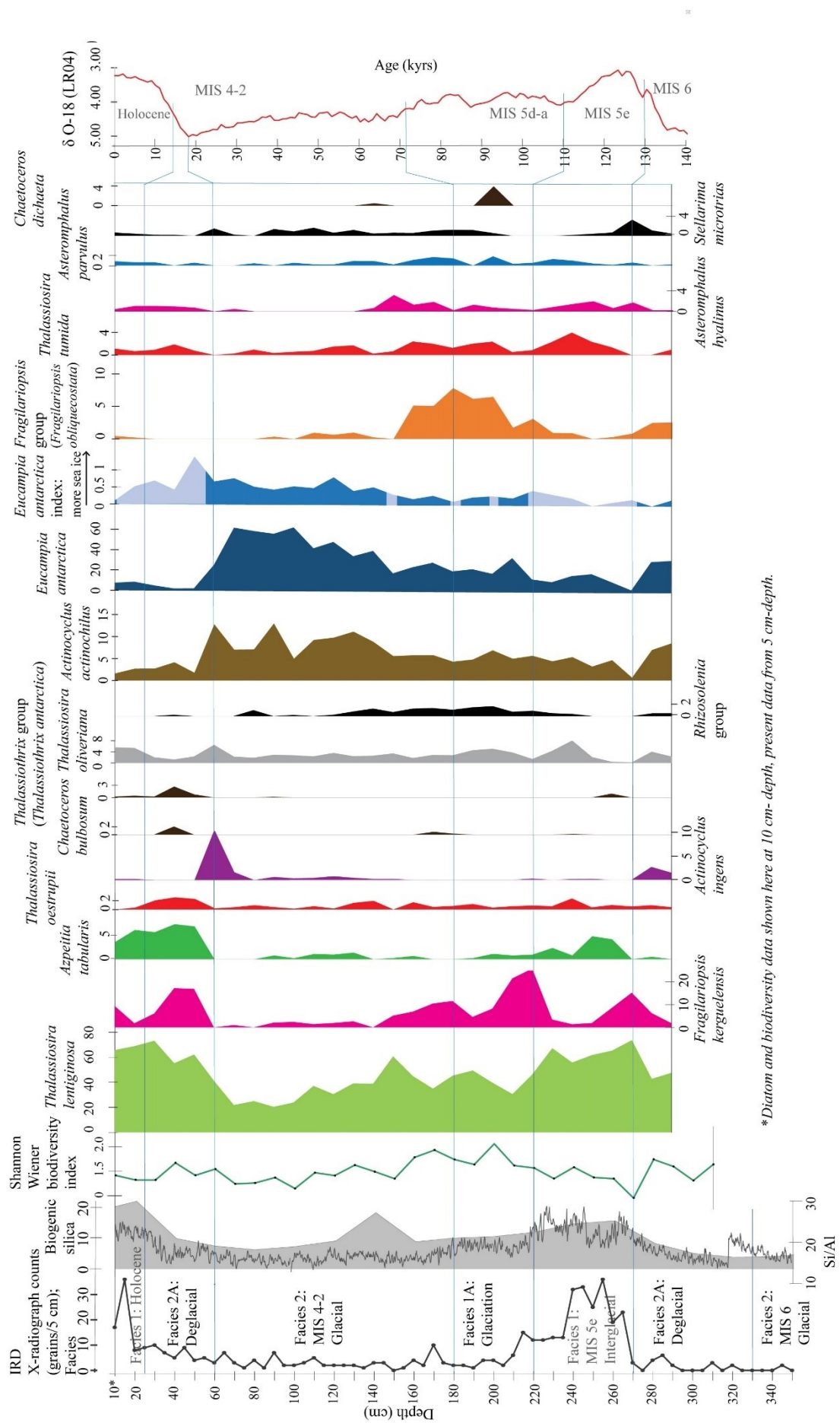
*Diatom and biodiversity data shown here at 10 cm- depth, present data from 5 cm-depth.

490 **Figure 3**-Tan_44 distribution of main species, species groups and *Eucampia* ~~terminal/ intercalary (T/I)~~ index (Terminal/ Intercalary valve ratio~~.~~). Results include ~~valve~~IRD counts ~~(per slide)~~, facies interpretation (vertical lines), biogenic silica (%), Si/Al (XRF) and the Shannon-Wiener biodiversity index. The facies model is shown, in comparison to LR04 (Lisiecki & Raymo 2005). Species in black are not included in statistical analysis due ~~~~to lower abundance (>1.82% in just one sample)~~ *Rhizosolenia* group (mainly Rhizosolenia *styliformis* and
495 *Rhizosolenia* (twin process) *antennata, ~~Chaetoceros.bulbosum,~~ Thalassiothrix* group (mainly *Thalassiothrix antarctica), Stellarima microtrias, Chaetoceros bulbosum,* and *Chaetoceros dichaeta*. *Eucampia* index was also not included in statistical analysis.

3.~~3~~ 4 Cluster and principal component analyses
500

Cluster analysis groups samples~~,~~ according to the similarity of the sample assemblages (Shi 1993). The groupings, illustrated by a dendrogram, can represent similar environments, and therefore aid in the reconstructions of paleoenvironments. Based on the relative abundance of diatom species and *Fragilariopsis* ~~species~~ group~~s~~, ~~three~~ four clusters were identified (Fig. 4), with a dissimilarity index of 4~~~~7%. The two largest
505 groups, Cluster 1 and Cluster 2, correlate well with the interglacial and glacial facies, respectively (Fig. 4).

Cluster 1 includes samples from 5~~-~~ 50 cm, 150 cm, ~~210 110 cm~~ and ~~290~~270~~-230~~ 220 cm. This cluster, which contains open ocean species (Fig. 3), is associated with mainly the interglacial, deglacial and much less with glacial facies. Cluster 2 includes samples from 140-~~60~~110 cm, 200- 160 cm, and 60 cm. This cluster is mainly
510 associated with the glacial facies, represented by sea ice and ice edge species (Fig. 3). Cluster 3~~, which~~ includes samples from ~~50 20 cm and 220 cm~~100-70 cm and~~,~~ is associated with the glacial facies. Cluster 4 is represented by only one sample, at 4~~, deglacial interval and includes~~ 210 cm ~~interval, associated~~ within the glaciation facies.~~, is~~and ~~represented by *Thalassiosira lentiginosa* and *Fragilariopsis kerguelensis* but also includes increase in *Fragilariopsis* group species.~~
515

The Q-mode PCA analysis identified ~~four~~three components that together explained 5~~2~~54% of sample variance (Table ~~S3~~S2; Table ~~2~~3). Component 1 (PC 1) explains 1~~8~~26% of the variance and contains contributor species associated with open ocean and sea ice edge environments. Species determining this component are *Thalassiosira lentiginosa, Actinocyclus actinochilus, Eucampia antarctica, Azpeitia tabularis,* and
520 *Asteromphalus hyalinus.* Component 2 (PC 2) explains 16% of the variance and is associated with sea ice or the coastal Antarctic environment. These are the *Fragilariopsis* group (dominated by *Fragilariopsis obliquecostata), Asteromphalus parvulus,* ~~the *Rhizosolenia* group (dominated by *Rhizosolenia styliformis),*~~ and *Thalassiosira tumida~~, and Chaetoceros dichaeta~~.* Component 3 (PC 3) explains ~~8.6~~12% of the variance and its contributor species are associated with open ocean environment. These are *Actinocyclus ingens, Actinocyclus*
525 *actinochilus,* and *Thalassiosira ~~oliverana~~oliveriana~~, and Fragilariopsis kerguelensis~~.* ~~Component 4 (PC 4) explains 8.69% of the variance and its contributor species are~~is associated with the open ocean~~, high nutrient, and warmer ocean~~ environment~~s~~. ~~These are the~~It comprises of *~~Fragilariopsis kerguelensis, Thalassiothrix group, Chaetoceros bulbosum,~~ and ~~Eucampia antarctica~~.*

530 R-mode PCA analysis identified ~~four~~three ~~main~~components, explaining 99% of the down core variance (Table ~~S4~~S3; Fig. 5). The variance is mostly explained by PC 1 and PC 2.~~, with PC 3 explaining <20% and PC 4 <2%~~

~~of the variance~~. PC 1, the open ocean assemblage, explains ~~43~~54% of the variance and shows high factor loadings at 40-5 cm and 270-150 cm. ~~the .~~ Both of these intervals coincide with Cluster 1, 2 and ~~3~~4, in the interglacial, deglacial, glaciation and early MIS 4-2 glacial facies. PC 2, the sea ice, and ice-edge species assemblage (Table ~~2~~3), explains ~~36~~42% of the variance and shows high factor loadings at 140-~~60~~70 cm, 170 cm, 210 cm, and 290-280 cm. These intervals coincide with Cluster 2 and 3, in the glacial facies and Cluster 4~~1~~ in the ~~early MIS 4-2 glacial,~~ glaciation ~~and deglacial~~ facies (Fig. 5). ~~PC 3, the reworked assemblage explains 19% of the variance and shows high factor loadings at 60-20 cm, 230-220 cm, and 270 cm intervals. These intervals coincide with Cluster 3, and Cluster 1 (sample 270 cm), in the deglacial, interglacial, and glaciation facies. PC 4, the high nutrient, warmer, open ocean assemblage, explains 1.4% of the variance, and~~ ~~has elevated factor loading at 40-60 cm, 180-160 cm, 220-210 cm, and 280-270 cm, in the deglacial, early glacial, and glaciation facies.~~
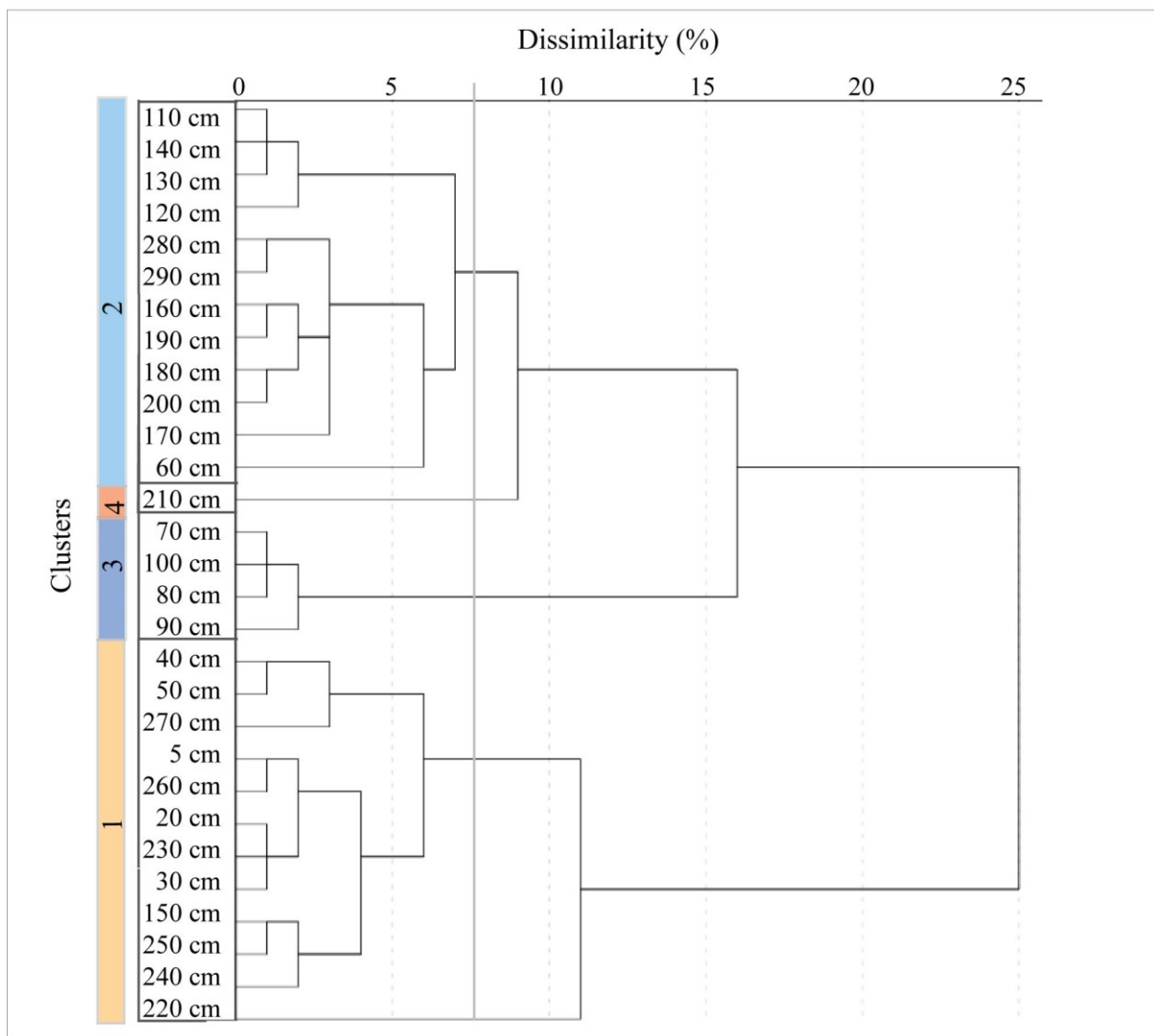
Figure 4 Hierarchical cluster analysis dendrogram illustrating agglomeration of four clusters at dissimilarity of ~~8~~7%.

Factor loadings	Assemblage	Environment
	P 1	
>0.5/ >-0.5	*Thalassiosira lentiginosa*	Open ocean
	Eucampia antarctica	
	Azpeitia tabularis	
	Astermophalus hyalinus	
	Actinocyclus actinochilus	Sea ice edge
	P 2	
>0.5	*Fragilariopsis* group*	Sea ice
	Thalassiosira tumida	Ice edge
	Asteromphalus parvulus	Coastal
	P 3	
>0.5	*Actinocyclus ingens*	Reworked
	Actinocyclus actinochilus	
	Thalassiosira oliverana	

* mainly *F .obliquecostata*

550

.

3.4 5 Correlation between diatom assemblages and productivity

555

~~Regression~~ Correlation analysis shows a strong statistical relationship between PC 1 and PC 2 assemblages, and Si/Al and biogenic silica (~~BSi), with r² values ranging from 0.2-0.5 (~~Table 34). PC 1 assemblage shows a positive correlation to Si/Al (~~PC 1=-0.32+(0.49 x Si/Al)~~r=0.63), and to biogenic silica (~~PC 1=0.33+(0.23 x BSi)~~r=0.57). PC 2 shows a negative correlation to Si/Al (~~PC 2=1.66+(0.06 x Si/Al)~~r=-0.62) and to biogenic silica (~~PC 2=0.87+(0.03 x~~r=-0.54 ~~BSi)~~). ~~In contrast, PC 3 and PC 4 assemblages have no correlation with either both Si/Al andor biogenic silica, showing r² values <0.1. The p values suggest the correlation between PC 1 and PC 2 and Si/Al or biogenic silica are significant~~All correlations are statistically significant (p < 0.001).

Table 34 Correlation (r²) between each PC component~~s~~ and Si/Al and biogenic silica~~.~~.

	r value	
Assemblage	Si/Al	Biogenic silca
PC 1 open ocean	0.63*	0.57*
PC 2 sea ice	-0.62*	-0.54*

* statistically significant correlation (p < 0.001)

565
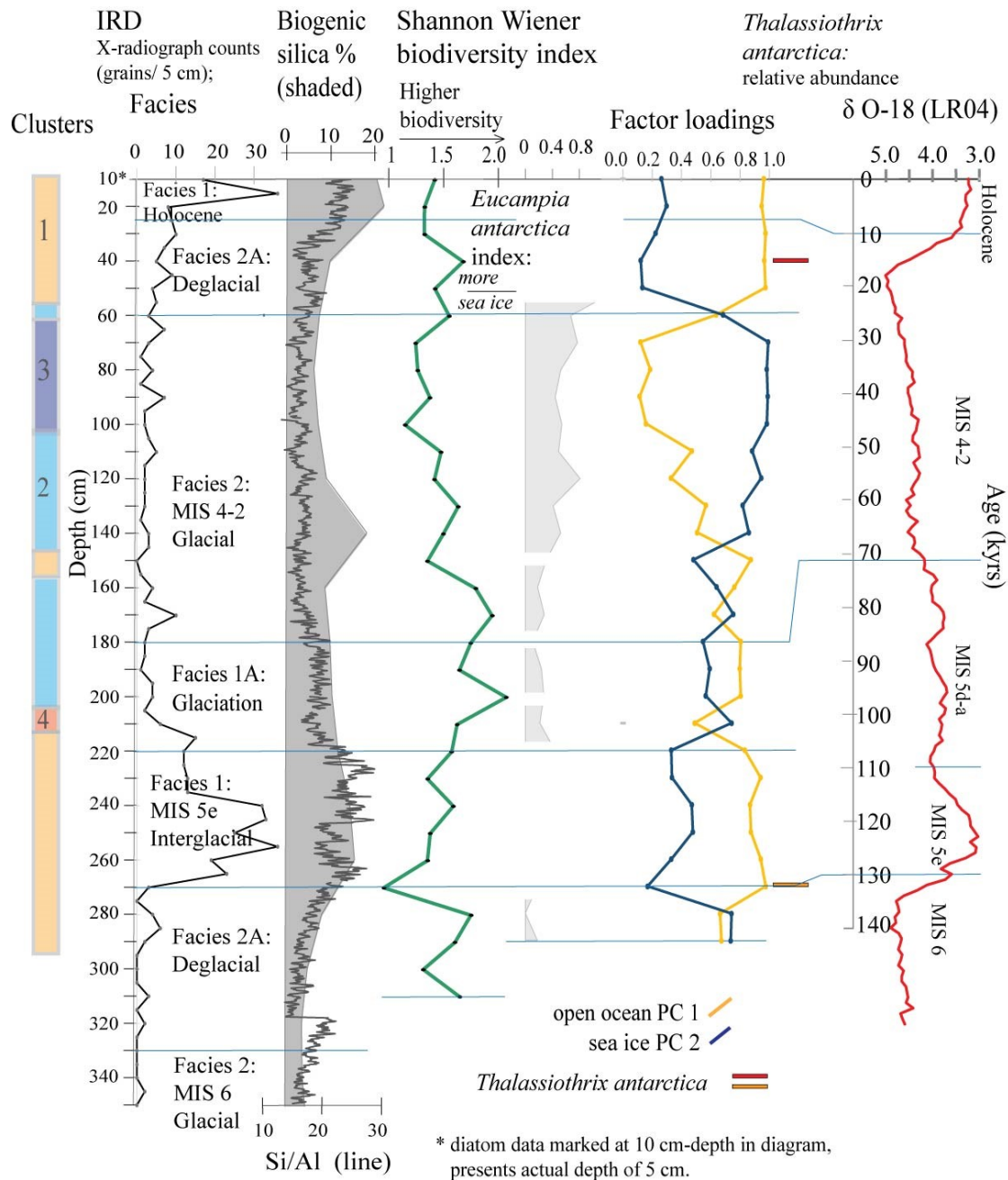
Figure 5 Principal Component (PC 1 and PC 4 2) factor loadings down core Tan_44, *Eucampia* index, *Thalassiothrix antarctica,* and Shannon-Wiener biodiversity index (green). Shaded areas show intervals of high factor loadings (dominance) of the assemblages and, of higher biodiversity. Also included are cluster results, IRD counts, sediment facies (horizontal lines), biogenic silica, Si/Al and LR04 curve (Lisiecki & Raymo 2005). *Eucampia* index results are presented here only at depths where total *Eucampia antarctica* counts >100 valves per sample. *Thalassiothrix antarctica* (red and orange) show depths with abundant broken valves, where 270 cm sample (orange) comprised 0% relative abundance of counted, valve ends.

4 Discussion

4.1 Diatom assemblages, clusters, and sedimentary facies

Principal component analysis distinguished ~~four diatom~~ 3 diatom assemblages. PC 1 and PC 2 assemblages incorporated most of the variance (42-54%), while PC 3 ~~and PC 4 were~~was much less influential (accounting for ~2% of total variance) ~~(Fig. 5). The assemblages and their environmental interpretation are described below. Due to PC 3 contributing a minor amount of variance to the samples, it is defined here, but it's not used in the environmental interpretations. Separately from the statistics, the *Eucampia* index and the presence of lower abundances indicator species, in particular the *Thalassiothrix* group – which indicates high productivity, are further discussed.

4.1.1 The open ocean assemblage (PC 1)

The PC 1 assemblage comprises open ocean species, *Thalassiosira lentiginosa*, *Eucampia antarctica*, and *~~Fragilariopsis kerguelensis~~Asteromphalus hyalinus* (Johansen and Fryxell 1985; Garrison and Buck 1989; Medlin and Priddle 1990; Zielinski and Gersonde 1997); ice edge species, *Actinocyclus actinochilus* (Medlin and Priddle 1990; Ligowski, Godlewski and Lukowski 1992; Garrison and Buck 1989; Armand et al. 2005), and warmer water species, *Azpeitia tabularis* (Zielinski and Gersonde 1997; Romero et al. 2005). Therefore, the PC 1 assemblage is interpreted to represent an open ocean environment, relatively warmer ocean, with a seasonal sea ice cover (Table ~~2~~3), and high productivity ~~environments,~~ similar to the modern-day environment over the core site.

The composition of the PC 1 assemblage further suggests that selective species preservation, due to reworking by bottom currents and/or dissolution processes, had been active. The presence of a combination of robust species, e.g., *Eucampia antarctica*, *~~Fragilariopsis kerguelensis,~~* and *Actinocyclus actinochilus,* suggests that some level of reworking of sediments influenced the assemblage composition (Shemesh, Burckle, and Froelich, 1989; Taylor and McMinn 1997). These species have been found within assemblages considered to have been influenced by reworking off Cape Darnley in Prydz Bay (Taylor and McMinn 1997) and the continental slope of the Ross Sea (Truesdale and Kellogg 1979). Reworking is corroborated by the knowledge that the site is currently influenced by the down slope flow of Adélie AABW and along slope currents, including the ASF (Fig. 1; Williams et al. 2008). Furthermore, the presence of unusual abundances of *Thalassiosira lentiginosa* (Fig. 3), a species usually associated with open ocean assemblages (Taylor and McMinn 1997; Truesdale and Kellogg 1979; Crosta et al. 2005) has been associated with dissolution (Shemesh, Burckle, and Froelich, 1989) suggest~~ings~~ that there is some level of dissolution affecting the PC 1 assemblage composition ~~(Shemesh, Burckle, and Froelich, 1989)~~. Such high abundances of *T. lentiginosa* are not observed in modern sediments in the Adélie region (Leventer 1992), or elsewhere within the sea ice zone on the Antarctic margin (Zielinski and Gersonde 1997; Armand et al. 2005; Crosta et al. 2005). Despite the influence of reworking and dissolution, the PC 1 assemblage is still considered to be primarily autochthonous and dominated by *in-situ* deposition associated with open ocean, warmer water, and sea ice edge species. The presence of *Azpeitia tabularis,* a~~nd~~ *Asteromphalus hyalinus,* species not commonly associated with reworking or dissolution, further confirms this position.

4.1.2 The sea ice assemblage (PC 2)

The largest contributions to the PC 2 assemblage (Table ~~2~~3) are from the *Fragilariopsis* group, comprising

620   mainly *Fragilariopsis obliquecostata*, a species which currently lives in sea ice and at the sea ice edge
(Ligowski, Godlewski & Lukowski 1992; Medlin & Priddle 1990; Moisan & Fryxell 1993). In Antarctic
continental margin surface sediments from the Ross Sea, Weddell Sea and Prydz Bay, *Fragilariopsis*
obliquecostata appears where sea ice cover is present >7 months per year (Armand et al. 2005). Other species
in PC 2 include the coastal species, *Asteromphalus parvulu*s (Kopczynska et al. 1986; Scott and Thomas 2005),

625   ~~cool open ocean species, the *Rhizosolenia* group, comprising mainly *Rhizosolenia styliformis*,~~ and the open
water/ sea ice edge species *Thalassiosira tumida* (Garrison & Buck 1989) ~~and the coastal and sea ice edge~~
~~species *Chaetoceros dichaeta* (Beans et al. 2008; Kopczynska, Weber & El Sayed 1986; Ligowski 1983). This~~
~~interpretation is further supported by the *Eucampia antarctica* terminal/ intercalary ratio, a sea ice and sea ice~~
~~edge proxy (Fryxell 1991), with values generally ranging from 0.0-0.8 (Fig. 3).~~ Based on a combination of sea

630   ice and sea ice edge/ coastal species, the PC 2 assemblage is interpreted as resulting from an environment
proximal to the permanent sea ice edge with a long sea ice duration of >7 months, as currently observed in the
Ross and Weddell Seas (Fetterer et al. 2017).

635   **4.1.3 The reworked assemblage (PC 3)**

The PC 3 assemblage comprises *Actinocyclus ingens*, *Actinocyclus actinochilu* and~~s,~~ *Thalassiosira*
~~*oliverana*~~*oliveriana*~~, and *Fragilariopsis*~~ kerguelensis (Table 3). *Actinocyclus ingens* is an extinct species,
~~associated~~ with LAD 0.~~65-1.25 M old sediments (Harwood~~43-0.5 Ma (Cody et al. ~~1992~~2008). *Thalassiosira*

640   ~~*oliverana*~~*oliveriana*~~ and *Fragilariopsis kerguelensis* are~~is a species associated with open ocean environments
(Medlin and Priddle 1990~~; Kopczynska 1986; Garrison and Buck 1989~~), while *Actinocyclus actinochilus* is
associated with sea ice edge environments (Medlin and Priddle 1990; Garrison and Buck 1989). However, these
species (~~except~~including *A. ingens*) have robust valves that can survive transport by bottom currents (Shemesh,
Burckle & Froelich 1989; Taylor and McMinn 1997; Truesdale and Kellogg 1977). PC 3 is therefore interpreted

645   as a reworked assemblage (allochthonous), transported from elsewhere by bottom water transport, with no *in*
situ deposition, and hence no environmental signal. The reworking is supported by the presence of extinct
Actinocyclus ingens, which ~~is an extinct species and was probably transported to Tan_44 from older sediments~~
~~on the margin. *Actinocyclus ingens*~~ is only found at 60 cm and 290-280 cm depth (Fig. 3). The 60 cm interval
also contains pyritised shells (Fig. S1). Due to its very small influence on variability, the PC 3 assemblage is not

650   considered further in the paleoenvironmental interpretation of Tan_44.

4.1.4 ~~The high productivity assemblage (PC 4)~~*Thalassiothrix antarctica* – a high productivity proxy

~~This assemblage includes *Fragilariopsis kerguelensis,* the~~Aside from statistical analysis, the down core

655   distribution of the *Thalassiothrix* group, of which *Thalassiothrix antarctica* is the most common species, are

considered as environmental indicators (Fig. 3; Fig. 5). ~~, is considered in this core as a strong environmental proxy, because it~~ is ~~found in great visual abundance in sediments, at 40 cm and 270 cm~~ (Fig. 5~~5~~; Fig. 3). ~~,~~ ~~*Chaetoceros*~~ *Thalassiothrix antarctica,* as well as the other two species which make up this group, *Thalassiosira lentiginosa* and *Trichotoxon reinboldii,* are open ocean species ~~bulbosum and *Eucampia antarctica*~~ (Table 2). ~~*Fragilariopsis kerguelensis* and *Eucampia antarctica* are open ocean species~~ (Kopczynska 1998; Garrison and Buck 1989; Beans et al. 2009). *Thalassiothrix antarctica* ~~is~~and *Thalassiothrix longissima* are ~~-~~found in ~~abundance in~~ surface sediments, between coastal Antarctica and the subtropical front (Zielinski and Gersonde 1997~~; Crosta et al. 2005~~). While~~,~~ *Trixotoxon reinboldii* is associated with sediment from colder/ ice edge waters (Crosta et al. 2005), *Thalassiothrix antarctica* is also associated with diatom blooms that occur in modern coastal and shelf waters, such as in Prydz Bay (Ligowski 1983; Quilty et al. 1985) or in naturally fertilised areas, such as the Kerguelen Plateau (Rembauville et al. 2015). ~~*Chaetoceros bulbosum* is found in the open ocean, generally south of the Polar Front (Kopczynska 1998).~~ Zielinski and Gersonde (1997) consider *Thalassiothrix antarctica* ~~and *Chaetoceros* species~~ from the Weddell Sea sediments to be indicators of high productivity. *Thalassiothrix antarctica* is not found in modern sediments off Adélie region~~,~~ ~~where only *Chaetoceros* blooms are evident~~ (Leventer 1992). However, Beans et al. (2009) found that this species can sometimes be abundant in waters off~~shore~~ Adélie Land. Based on the conclusions of Zielinski and Gersonde (1997) and Rembauville et al. (2015), ~~the PC 4 assemblage is suggested to be~~the abundance of the *Thalassiothrix* ~~*antarctica,*~~ group, represented largely by *Thalassiothrix antarctica* species, ~~are~~is indicative of a higher nutrient environment and higher productivity than in the present Adélie region, which we associate~~d~~ with . ~~Thus, the PC 4 assemblage is considered indicative of high nutrient input and~~increased upwelling of ~~warm water~~the Circumpolar Deep Water.

~~represents overvalve ratio of species, and its increase is associated with   in the environment. In (Fryxell 1991); Fig. 5 high index considered in due to~~

4.2 Palaeoecological interpretation

4.2.1 Interglacial (MIS 5e and Holocene)

The interglacial facies is associated with PC 1 (open ocean assemblage; Fig. 5; Table ~~2~~3), and to a lesser extent with PC 2 (sea ice assemblage). The dominance of the PC 1 assemblage suggests that the Holocene and MIS 5e environments had seasonal sea ice, with open ocean (during the summer) and sea ice cover (during winter, spring, and autumn), similar to the modern situation (Fig. 1). The inference of the seasonal presence of sea ice is strengthened with the moderate presence of PC 2 assemblage, which represents increased sea ice duration. PC 1 also provides evidence of reworked and a dissolution-affected assemblage. Indeed, strong bottom currents, such as AABW, and ASF, which sweep the continental slope off~~shore~~ Adélie Land~~,~~ at present (Fig. 1; Williams et al. 2010), may have been active throughout the Holocene and MIS 5e. Furthermore, the reworking by bottom

currents may have been stronger at times. This is further suggested by the slight presence of PC 3, which represents reworked assemblages. Lastly, the PC 1 assemblage is associated with elevated productivity, which is supported by high Si/Al and biogenic silica, but lower biodiversity (Fig. 5). Low biodiversity is likely affected by poor preservation (dissolution and reworking), but potentially also reflects modern diatom blooms, which are typically of lower biodiversity (Beans et al. 2008). The close similarity of diatom assemblages between the two interglacial facies, MIS 5e and Holocene, suggests that ocean temperature, circulation, and seasonal sea ice duration in the Adélie region were similar during these two interglacial periods (Fig. 5).

4.2.2 Glaciation MIS 5d-5a (interglacial to glacial transition)

The glaciation facies shows clear evidence for an increase in the influence of sea-ice over the core site~~,~~ compared to the interglacial facies. The PC 2 assemblage starts to increase at this time, and the *Eucampia* index increases slightly ~~from the low~~ over MIS5e values (Fig. 5). ~~The glaciation facies~~ *F.~~rag~~ kergulensis* reach maximum abundance early in the glaciation (Fig. 3), while the abundance of *Fragilariopsis* group (dominated by *F. obliquecosta*) increases strongly throughout the glaciation, reaching a maximum abundance at the transition to MIS 4-2 (Fig. 3). ~~is associated with high PC 1 open ocean assemblage. The early glaciation facies is associated with an increase in~~d PC 2 (sea ice assemblage)~~, increase in *Fragilariopsis* group, and the *Eucampia* index (Fig. 5)~~ and a minor increase in PC 4 (high productivity assemblage)~~and high PC 1 assemblage, while the late glaciation is associated with increasing PC 1 (open ocean assemblage), a gradually~~lower decreasing PC 2 ~~and a minor increase in PC 4 (Fig. 5)~~ of which *Fragilariopsis* ~~species are part of, even though the down core distribution of *Fragilariopsis* group, with *Fragilariopsis obliquecostata* suggest late glaciation also has substantial sea ice increase.~~ . The increase in PC 2 ~~and *Fragilariopsis* group,~~ in the early glaciation, relative to the MIS 5e interglacial, therefore suggests that the sea ice season initially increased in duration, in response to cooling. ~~This is coupled with periods of slightly elevated PC 4 suggesting intervals of elevated nutrient input and warmer water influx, potentially reflecting periods of increased rates of CDW upwelling, relative to the present day. Although PC4 is a minor component of the diatom assemblage, the presence of both elevated PC 4 and PC 2 (Fig. 5), suggests both an increase of sea ice (and thus cooling) and a warm water influx, occurred over the Adélie region during the early glaciation stage. This may have occurred during different seasons, i.e., the sea ice season may have increased over autumn, winter, and spring, while CDW influx may have increased during summer.~~ F~~urthermore~~inally, the *Rhizosolenia* group, of which the cold-water species *Rhizosolenia styliformis* (Fig. 3) dominate, ~~are found throughout ~~the glaciation facies. Together, the PC 2 assemblage, ~~the sea ice and cold water species~~*Fragilariopsis* species, *Eucampia* index, and *Rhizosolenia styliformis*~~ suggest that the ~~entire~~glaciation facies was characterised by an~~, contained ~~increase in the ~~d~~ sea ice season, relative to the MIS 5e interglacial.

The productivity proxies, Si/Al, and biogenic silica are low, indicating a decrease in productivity throughout the glaciation (Fig. 5). However, the opposite is indicated by the continued presence of PC 1, which suggests high productivity.

The Shannon Wiener index suggests that the late glaciation ~~(like the early glacial, MIS 4-2)~~ was a time of relatively high biodiversity (Fig. 5) relative to the MIS 5e and Holocene interglacials. This may be due to a more diversified environment, that is, the increased sea ice season, and times of ~~increased CDW influx~~open water may have produced a more diversified community. ~~Interestingly, the early glaciation, also characterised by elevated PC 2 and PC 4, is associated with lower biodiversity.~~ In the modern shelf environment, a greater diatom biodiversity is found near the Astrolabe Glacier, rather than near the Mertz Glacier, where productivity is higher, yet dominated by fewer species (Beans et al. 2008). Thus, the biodiversity in the samples may reflect this natural variability seen in the diatom assemblages in the Adélie region today.

4.2.3 Glacial (MIS 4-2)

Diatom assemblages can be used to subdivide the MIS 4-2 glacial interval into early and late glacial stages (Fig. 5). The early glacial stage, comprising increased ~~high~~ loadings of PC 1 (open ocean assemblage) and increas~~ed~~ing loadings of PC 2 (sea ice assemblage), is similar to the glaciation, suggesting an initially prolonged sea ice season relative to the interglacial periods. The *Fragilariopsis* group is at its maximum in the early glacial stage (Fig. 3). ~~The early glacial stage also contains assemblages aligned with PC 4, suggesting an increased rate of CDW influx, and periods of increased seasonal blooms. The diatom assemblages at the start of the glacial have a higher biodiversity, similar to the glaciation stage. This likely reflects the diversity of assemblages including sea ice (PC 2) and open ocean (PC 1)~~high productivity (PC 4). After this initial increase in PC 2 ~~and PC 4~~, the assemblages align with high PC 1 only, suggesting temporary reversal of cooling, and an increase in productivity. ~~Although the PC 1 shows evidence of increased/ high productivity, the other productivity proxies, Si/Al, and biogenic silica show the opposite, that the O~~overall glacial productivity in this region was low with low Si/Al and biogenic silica. This is consistent with data from the broader Antarctic margin data (Bonn et al. 1998) and ~~from~~ with the glaciation and deglacial facies. ~~The reason for these opposing productivity signals is not clear, however, Hartman et al. (2021) also found similar results, with a low biogenic silica and Ba signal, yet an increase in Chaetoceros resting spores and Eucampia antarctica valves within the glacial record off Cape Adare (Ross Sea).~~ In the late glacial, from ~~150~~160-100 cm, the assemblage ~~aligns with~~displays a gradual increase in PC 2 ~~and a decrease in PC 1~~, suggesting ~~a gradual~~an increase in the duration of the sea ice season (Fig. 5). After this~~In the late glacial stage~~, from 100-70 cm, the assemblages align with high PC 2, the sea ice assemblage, suggesting maximum duration of the sea ice season occurred ~~during the~~towards the end of the late glacial stage (MIS 2). The increase in sea ice is further supporte~~d d,~~ by the increase in the *Eucampia* index (Fig. 5)~~, although the presence of PC 1 indicates that there was still a short period of time each summer when sea ice was not present~~.

The similarities in diatom assemblages between glaciation and early glacial stage suggests cooling of the ocean started long before the onset of the glacial and then continued ~~slowly (increasing~~ gradually ~~with the exception of a period of warming during the late glaciation stage)~~ until the maximum ~~cooling~~sea ice duration (and therefore, cooling) was reached, at the end of the last glacial (Fig. 5). This is consistent with gradual cooling reaching a maximum at the end of MIS 2, as seen in Antarctic ice cores (Jouzel et al. 1993) and Sea Surface Temperatures

 from global sediment cores (Kohfeld & Chase 2017), including records based on diatom assemblages from the Southern Ocean north ~~at~~ of 56 °S (Crosta et al. 2004; Chadwick et al. 2022). The assemblage

775 composition of the late glacial stage is suggestive of a long sea ice season duration, an environment which at present occurs in the Ross and Weddell Seas (Truesdale & Kellogg 1979; Zielinski & Gersonde 1997). This suggests that the permanent/ summer sea ice edge, during the late glacial stage, was closer to the core site than it is today, indicating that the core site was covered by near permanent sea ice during the peak glacial. However, the persistent presence of the *Thalassiosira lentiginosa* and PC 1, ~~though at lower levels,~~ provides evidence that

780 open ocean conditions existed over the Tan_44 site~~,~~ during part of the year.

4.2.4 Deglacials (glacial to interglacial transitions): MIS 2 to Holocene and MIS 6 to MIS 5e

The deglacial facies (between MIS 6 to MIS 5e and MIS 2 to Holocene)~~,~~ is generally associated with an increase

785 in PC 1 (open ocean assemblage)~~,~~ and a decrease in PC 2 (sea ice assemblage)~~,~~ relative to the glacial (Fig. 5). ~~PC 3 (reworked assemblage) is increased throughout the entire MIS 2 to the Holocene deglacial, and at the beginning and the end of the MIS 6 to MIS 5e deglacial, while PC 4 (high productivity assemblage) is slightly increased during both deglacials~~. The dominance of PC 1 suggests that there was ~~an increase~~high in productivity throughout the deglacial, although the productivity proxies, biogenic silica, and Si/Al, are low. The minor

790 influence of ~~PC 4~~ *Thalassiothrix antarctica* (at 40 cm; Fig. 5), relative to the glacial period, suggests an increase in CDW~~, relative to the glacial period~~ occurred after the decline of sea ice (at 60 cm, at end of the last glacial; Fig. 5) and prior to ice sheet retreat (at 15 cm, during the Holocene; Fig. 5). A similar sequence is observed within the MIS 6 to MIS 5e deglacial, but it is less clear. Here (at 270 cm; Fig. 5), the broken valves are abundant, but relative abundance is 0%, Tolotti et al. (2013), and Li et al. (2021), also suggest, based on the

795 presence of diatom species, that increased CDW influx occurred during the last deglacial in the Ross Sea and offshore Enderby Land, respectively. Lastly, the start of the MIS 2/1 deglacial (and end of MIS 6/5 deglacial) is marked by ~~the rapid~~a decrease in the PC 2 assemblage (Fig. 5), which suggests that the sea ice season duration ~~rapidly~~ declined rapidly at the end of the last glacial. This is consistent with the rapid sea ice retreat for the last two deglacial transitions from distal Southern Ocean (at 56°S) documented by Crosta et al. (2004) and

800 Chadwick et al. (2022).

In conclusion, the duration of the sea ice season ~~duration~~ decreased~~ occurred~~ relatively rapidly, and prior to CDW increase as evidenced by ~~the increase in PC 4 between~~*Thalassiothrix antarctica* ~~50~~ 40 cm ~~depth~~ (Fig. 5). this in turn occurred before the onset of ice sheet retreat (as indicated by IRD; Fig. 5). ~~Therefore, something~~

805 ~~other than increase in CDW influx influenced sea ice retreat.~~ However, a more detailed study of diatom assemblages is needed in order to determine the relative timing and a more detailed chronology of these deglacial changes.

4.2.5 Diatom barren MIS 6 glacial and ~~relatively low diatom~~micropyrite in MIS 6 to MIS 5e deglacial
810

The 350-320 cm interval is considered diatom barren, ~~having 7-22 valves per slide, while the 310-300 cm~~ ~~interval has a low relative diatom count of 88-245 valves per slide (Fig. 3; Table S5). Both of these intervals~~ ~~suggest a different environment in the late MIS 6 glacial and early MIS 6/5e deglacial compared to the 290-0 cm~~ ~~interval described and statistically analysed above. The diatom barren interval at 350-320 cm, and relatively low~~

LEGEND: ⊛ Productivity ▭▭▭ Sea ice season duration
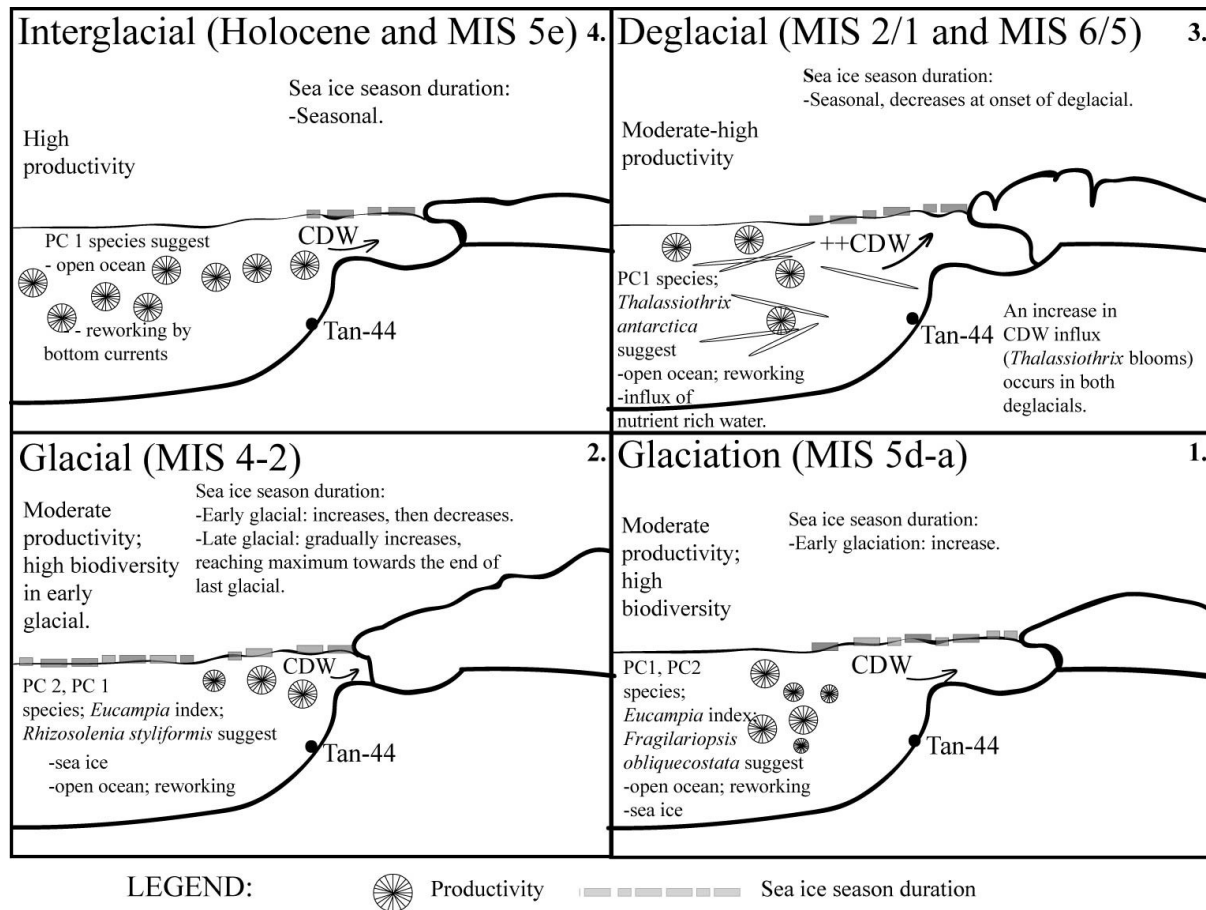
~~diatom interval at 310-300 cm,~~ (Table S4). ~~It~~This may be due to the original assemblage having been affected by dilution at the sea floor by turbidity currents (Kellogg & Truesdale 1979; Schrader et al. 1993; Escutia et al. 2003), or by a permanent sea ice cover, which reduced productivity allowing only reworked diatoms to be transported to the site by bottom currents (Table ~~S5~~S4). The presence of micropyrite within the 320-300 cm section suggests low oxygen levels could have prevailed during the time, brought on by either fast sedimentation, such as turbidity currents (Presti et al. 2011), or by an extensive sea ice cover (Lucchi et al. 2007). Interestingly, ~~pyrites are~~pyrite is also found ~~also~~ within the 80-60 cm section, which comprises an increase of the reworked assemblage (PC 3; Fig. 5) at the end of the MIS 4-2 glacial facies.

Figure 6 Sea ice and productivity interpretation across the last glacial cycle (~140- ~~~5ka~~~5 ka) based on diatom assemblage variability. During Holocene and MIS 5e interglacial periods, the seasonal sea ice cover at the site is similar to present-day. Sea ice cover duration initially increases then decreases in glaciation (MIS 5d-a); and early MIS 4-2 glacial. The sea ice then, gradually increases during late MIS 4-2 glacial, reaching a maximum seasonal duration towards ~~at~~the end of the last glacial. During the ~~early glacial, early glaciation and the end of~~ ~~glaciation (MIS 5d-a; i.e., last interglacial to glacial transition) and during the~~deglacials (i.e., last two glacial to interglacial transitions) the influx rate of CDW increased ~~for a period of time,~~relative to modern influx rates or other times, as suggested by the presence of the high nutrient~~/ warmer PC 4 assemblage~~species, *Thalassiothrix*

antarctica. This study suggests the sea ice decreased ~~rapidly~~ at the end of the last glacial, and that the increase in CDW influx occurred after the ~~retreat of~~ sea ice season declined, during the last deglacial. Yet, all of this occurred before the onset of the last major ice sheet retreat.~~.~~

5 Conclusion

Diatom assemblages in Tan_44 (64.5°S) varied on a glacial to interglacial timescale over the last 140 ~~k yrs~~kyrs, and their composition ~~was influenced by~~ reflects both *in situ* productivity, but is also influenced slightly by ~~and~~ bottom current reworking processes. ~~However, the~~The diatom assemblages were ~~mainly~~predominantly influenced by ~~environmental~~ changes ~~connected to~~in sea ice duration and changing ocean circulation over the core site. The following is a summary of conclusions reached in this study (Fig. 6):

- The PC 1 assemblage dominance in the interglacial facies suggests open ocean and seasonal sea ice environments during MIS 5e and Holocene, which are similar to today. The close correspondence of assemblages between the two interglacials suggests that both surface water conditions, related to sea surface temperature and sea ice duration were similar between the two interglacials.
- The unusually high dominance of *Thalassiosira lentiginosa* in the PC 1 assemblage in the interglacial facies suggests the assemblage was slightly affected by dissolution, and also by reworking by bottom currents.
- The duration of the sea ice season, as indicated by the presence of PC 2, started to increase during the early glaciation stage (MIS 5d-5a), and in the early MIS 4-2 glacial, and continued to increase throughout the late MIS 4-2 glacial, reaching a maximum extent towards the end of the glacial (MIS 2).
- However, T~~t~~he ~~presence of the PC 2 assemblage in the MIS 4-2 glacial facies suggests an environment with a long sea ice season. However, the~~ presence of both PC 2 and PC 1 assemblages during the MIS 4-2 glacial provides evidence that the summer sea ice edge was located further south than the core site,~~,~~ at 64.5°S~~,~~ in the Adélie region.
- ~~The duration of the sea ice season, as indicated by the presence of PC 2, started to increase during the early glaciation stage (MIS 5d-5a), and in the early MIS 4-2 glacial, and continued to increase throughout the late MIS 4-2 glacial, reaching a maximum extent towards the end of the glacial (MIS 2).~~
- The rapid ~~abrupt~~ decrease of the PC 2 sea ice assemblage ~~at the end of the last glacial,~~ suggests a ~~relatively rapid~~ decline in the sea ice season occurred at the end of the last glacial.
- ~~The glaciation stage and the early glacial are similar: they contain an initial increase in sea ice duration (PC 2). Furthermore, both glaciation and early glacial periods contain a slight influence of PC 4, suggesting an increased CDW influx occurred synchronously with the increase in sea ice duration. This may have occurred during different times of the year.~~
- ~~PC 1, PC 2, and PC 4 were expressed during climate transitions, that is, during the deglacial and glaciation.~~ *Thalassiothrix antarctica* was found to be ~~visually~~relativlely abundant in both deglacials, ~~This~~ suggest~~sing~~ ~~the presence of open water and increased seasonal sea ice environments but also periodic~~ an ~~-~~increase~~s~~ of

high nutrients and warmer water. This influx is, interpreted here as increase in upwelling of CDW in the Adélie region, during these times.

875   -   Based on the diatom assemblages and the IRD abundanceincrease in the Tan_44 core, the sea ice retreated prior to the increase in CDW upwelling during the last deglaciationl, and these were thenwhich was followed by an increase in IRD, indicating the retreat of the ice sheet.

   Biodiversity was highest during the glaciation stage and the start of the last glacial, and lowest during the late glacial and the interglacial periods. The higher biodiversity during glaciation and the start of the glacial
880   could be the result of a more diversified environment relative to other periods. This may have been due to increased CDW influx during the spring and summer, and an., perhaps due to an extended sea ice season during winter spring or autumn. The lower biodiversity during the glacial is likely due to a the overallmore increased sea ice season, relative to glaciation.

   -

885   This new diatom data set provides an understanding of the changes in sea ice proximal to East Antarctica over the last glacial cycle. It provides new insight into the extent of the summer sea ice in the last glacial, the winter sea ice extent during the last interglacial, and also suggests changes within seasonal sea ice with respect to the upwelling of CDW, during climate (glacial to interglacial) transitions. These are important parameters to constrain climate models to understand the importance of the influence of Antarctic Sea sea ice on global
890   climate over the last 140 ka. Further marine sediment core and sea ice data (increased resolution and more cores) is required to improve our understanding of the spatial and temporal changes in sea ice proximal to Antarctica.

Data availability

895   The data is available at PANGAEA: https://doi.org/10.1594/PANGAEA.946549
   .

Competing interest

   The authors declare there is no conflict of interest in relation to work presented in this study and in the
900   Supplement.

Acknowledgements

This research was supported under Australian Research Council's Special Research Initiative for Antarctic Gateway Partnership (Project ID SR140300001). This research was funded as part of PhD studies, by Antarctic
905   Gateway Partnership at the Institute for Marine and Antarctic Studies (IMAS). We acknowledge National Institute of Water and Atmospheric Research (NIWA), Wellington, New Zealand and the crew and scientists from RV Tangaroa, from the 2013 voyage lead by Dr Mike Williams. This TAN1302 voyage was funded by New Zealand, Australia and French research agencies. The core was originally logged onboard ship by Dr Molly Patterson. Dr Taryn Noble assisted with u channel preparation at NIWA in Wellington, while the XRF
910   scanning was completed by Patricia Gadd at ANSTO laboratories in Sydney. We further acknowledge Dr Nils Jansen who assisted with biogenic silica analyses at IMAS, Lisa Northcote, who assisted in grain size analysis, and Geraldine Jacobs and Alan William at the Australian Nuclear Science and Technology (ANSTO) who

coordinated ^{14}C analysis. We also acknowledge the funding for 14C dating, provided by ANSTO Research Portal Proposal 10705.

915

References

Alley, R. B., Anandakrishnan, S., Christianson, K., Horgan, H. J., Muto, A., Parizek, B. R., Pollard, D. & Walker, R. T.: Oceanic forcing of ice-sheet retreat: West Antarctica and more, Annual Review of Earth and
920   Planetary Sciences, 43, 207-231, 2015.

Andrews, J. T., Domack, E. W., Cunningham, W. L., Leventer, A., Licht, K. J., Jull, A. T., DeMaster, D. J. and Jenningst, A. E.: Problems and possible solutions concerning radiocarbon dating of surface marine sediments, Ross Sea, Antarctica, Quaternary Research, 52, 2, 206-216, 1999.
925
Armand, L K., Crosta, X., Romero, O. and Pichon, J. J.: The biogeography of major diatom taxa in Southern Ocean sediments: 1. Sea ice related species, Palaeogeography, Palaeoclimatology, Palaeoecology, 223, 1-2, 93-126, 2005.

930   Arndt, JE, Schenke, HW, Jakobsson, M, Nitsche, FO, Buys, G, Goleby, B, Rebesco, M, Bohoyo, F, Hong, J, Black, J and Greku, R 2013, 'The International Bathymetric Chart of the Southern Ocean (IBCSO) Version 1.0—A new bathymetric compilation covering circum-Antarctic waters', *Geophysical Research Letters*, vol. 40, no. 12, pp.3111-3117.

935   Arrigo, K. R. and Van Dijken, G. L. 2003: Phytoplankton dynamics within 37 Antarctic coastal polynya systems, Journal of Geophysical Research: Oceans, 108, C8, 2003.

Beans, C., Hecq, J. H., Koubbi, P., Vallet, C., Wright, S. and Goffart, A.: A study of the diatom-dominated microplankton summer assemblages in coastal waters from Terre Adélie to the Mertz Glacier, East Antarctica
940   (139 E-145 E), Polar Biology, 31, 9, 1101-1117, 2008.

Bonn, W. J., Gingele, F. X., Grobe, H., Mackensen, A. and Fütterer, D. K.: Palaeoproductivity at the Antarctic continental margin: opal and barium records for the last 400 ka, Palaeogeography, Palaeoclimatoloy, Palaeoecology, 139, 3, 195-211, 1998.
945
Bodungen, B. V., Smetacek, V. S., Tilzer, M. M. and Zeitzschel, B.: Primary production and sedimentation during spring in the Antarctic Peninsula region, Deep Sea Research Part A. Oceanographic Research Papers, 33, 2, 177-194, 1986.

950   Burckle, L. H., Jacobs, S. S. and McLaughlin, R. B.: Late austral spring diatom distribution between New Zealand and the Ross Sea Ice Shelf, Antarctica: Hydrographic and sediment correlations, Micropaleontology, 74-81. 1987.

Burckle, L. H.: Ecology and palaeoecology of the marine diatom Eucampia antarctica (Castr.) Mangin, Marine
955   Micropaleontology, 9, 1, 77-86, 1984.

Busetti, M., Caburlotto, A., Armand, L., Damiani, D., Giorgetti, G., Lucchi, R. G., Quilty, P. G and Villa, G.: Plio-Quaternary sedimentation on the Wilkes Land continental rise: 'preliminary results', Deep Sea Research Part II: Topical Studies in Oceanography, 50, 8-9, 1529-1562, 2003.
960
Caburlotto, A., Lucchi, R. G., De Santis, L., Macri, P. and Tolotti, R.: Sedimentary processes on the Wilkes Land continental rise reflect changes in glacial dynamic and bottom water flow, International Journal of Earth Sciences, 99, 4, 909-926, 2010.

965   Caburlotto, A., De Santis, L., Zanolla, C., Camerlenghi, A. and Dix, J.: New insights into Quaternary glacial dynamic changes on the George V Land continental margin (East Antarctica), Quaternary Science Reviews, 25, 21, 3029-3049, 2006.

970 Chadwick, M., Crosta, X., Esper, O., Thöle, L. and Kohfeld, K.E., Compilation of Southern Ocean sea-ice records covering the last glacial-interglacial cycle (12–130 ka), *Climate of the Past Discussions*, 1-24, 2022.

Cody, R. D., Levy, R.H., Harwood, D.M. and Sadler, P.M.: Thinking outside the zone: High-resolution quantitative diatom biochronology for the Antarctic Neogene. Palaeogeography, Palaeoclimatology, Palaeoecology, 260, 92–121, 2008.

975

Cook, C. P., van de Flierdt, T., Williams, T., Hemming, S. R., Iwai, M., Kobayashi, M., Jimenez-Espejo, F. J., Escutia, C., González, J. J., Khim, B. K., McKay, R. M., Passchier, S., Bohaty, S. M., Riesselman, C. R., Tauxe, L., Sugisaki, S., Galindo, A. L., Patterson, M. O., Sangiorgi, F., Pierce, E. L., Brinkhuis, H., Klaus, A., Fehr, A., Bendle, J. A. P., Bijl, P. K., Carr, S. A., Dunbar, R. B., Flores, J. A., Hayden, T. G., Katsuki, K., Kong, G. S.,
980 Nakai, M., Olney, M. P., Pekar, S. F., Pross, J., Röhl, U., Sakai, T., Shrivastava, P. K., Stickley, C. E., Tuo, S., Welsh, K. and Yamane, M.: Dynamic behaviour of the East Antarctic ice sheet during Pliocene warmth, Nature Geoscience, 6, 765, 2013.

Cooke, D. W. and Hayes, J. D.: Estimates of Antarctic Ocean seasonal sea-ice cover during glacial intervals, Antarctic geoscience, 131, 1017-1025, 1982.

985

Crosta, X., Romero, O., Armand, L. K. and Pichon, J. J.: The biogeography of major diatom taxa in Southern Ocean sediments: 2. Open ocean related species, Palaeogeography, Palaeoclimatology, Palaeoecology, 223, 1-2, 66-92, 2005.

990 Crosta, X., Strum, A., Armand, L. K. and Pichon, J. J.: Late Quaternary sea ice history in the Indian sector of the Southern Ocean as recorded by diatom assemblages, Marine Micropaleontology, 50, 3, 209-223, 2004.

Crosta, X., Debret, M., Denis, D., Courty, M. A. and Ther, O.: Holocene long- and short-term climate changes off Adélie Land, East Antarctica, Geochemistry Geophysics Geosystems, 8, Q11009,
995 doi:10.1029/2007GC001718, 2007.

Crosta, X., Kohfeld, K. E., Bostock, H. C., Chadwick, M., Du Vivier, A., Esper, O., Etourneau, J., Jones, J., Leventer, A., Müller, J., Rhodes, R. H., Allen, C. S., Ghadi, P., Lamping, N., Lange, C., Lawler, K.-A., Lund, D., Marzocchi, A., Meissner, K. J., Menviel, L., Nair, A., Patterson, M., Pike, J., Prebble, J. G., Riesselman, C.,
1000 Sadatzki, H., Sime, L. C., Shukla, S. K., Thöle, L., Vorrath, M.-E., Xiao, W., Yang, J.: Antarctic sea ice over the past 130,000 years, Part 1: A review of what proxy records tell us, EGUsphere [preprint], https://doi.org/10.5194/egusphere-2022-99, 2022.

DeMaster, D. J.: The supply and accumulation of silica in the marine environment, Geochimica et
1005 Cosmochimica acta, 45, 10, 1715-1732, 1981.

Dennis, D., Crosta, X., Zaragosi, S., Romero, O., Martin, B. and Mas, V.: Seasonal and subseasonal climate changes recorded in laminated diatom ooze sediments, Adelie Land, East Antarctica, The Holocene, 16, 8, 1137-1147, 2006.
1010
Denis, D., Crosta, X., Barbara, L., Massé, G., Renssen, H., Ther, O. and Giraudeau, J.: Sea ice and wind variability during the Holocene in East Antarctica: insight on middle–high latitude coupling, *Quaternary Science Reviews*, *29,* 27-28, 3709-3719, 2010.

1015 Depoorter, MA, Bamber, J, Griggs, J, Lenaerts, JT, Ligtenberg, SR, van den Broeke, MR & Moholdt, G, 'Calving fluxes and basal melt rates of Antarctic ice shelves', *Nature*, vol. 502, no. 7469, pp. 89-92, 2013.

Diekmann, B., Fütterer, D., Grobe, H., Hillenbrand, C., Kuhn, G., Michels, K., Petschick, R. and Pirrung, M.: Terrigenous sediment supply in the polar to temperate South Atlantic: 'Land-ocean links of environmental
1020 changes during the late Quaternary, in The South Atlantic in the Late Quaternary', Springer, 375-399, 2003.

Domack, E.W.: Sedimentology of glacial and glacial marine deposits on the George V-Adelie continental shelf, East Antarctica, *Boreas*, 11, 1, 79-97, 1982.

1025   Domack, E., Jull, A.T., Anderson, J., Linick, T. & Williams, C.: 'Application of tandem accelerator mass-spectrometer dating to late Pleistocene-Holocene sediments of the East Antarctic continental shelf', *Quaternary Research*, 31, 2, 277-287, 1989.

Doucette, G. J. and Fryxell, G. A.: Thalassiosira antarctica (Bacillariophyceae): Vegetative and resting stage
1030   ultrastructure of an ice-related marine diatom, Polar Biology, 4, 2, 107-112, 1985.

Escutia, C., Warnke, D., Acton, G.D., Barcena, A., Burckle, L., Canals, M. & Frazee, C.S.: Sediment distribution and sedimentary processes across the Antarctic Wilkes Land margin during the Quaternary, *Deep Sea Research Part II: Topical Studies in Oceanography*, 50, 1481-1508, 2003.

1035

Fetterer, F, Knowles K, Meier WN, Savoie M, and Windnagel, AK 2017 updated daily, '*Sea Ice Index', Version 3*, Boulder, Colorado USA, NSIDC: National Snow and Ice Data Center,
doi: https://doi.org/10.7265/N5K072F8.

1040   Fink, D., Hotchkis, M., Hua, Q., Jacobsen, G., Smith, A. M., Zoppi, U., Child, D., Mifsud, C., van der Gaast, H. and Williams, A.: The antares AMS facility at ANSTO, Nuclear Instruments and Methods in Physics Research Section B: Beam Interactions with Materials and Atoms, 223, 109-115, 2004.

Fryxell, G.: Comparison of winter and summer growth stages of the diatom Eucampia antarctica from the Kerguelen Plateau and south of the Antarctic convergence zone, Proc. ODP. Sci. Results, 119, 675-685, 1991.
1045

Fryxell, G. and Prasad, A.: Eucampia antarctica var. recta (Mangin) stat. nov. (Biddulphiaceae, Bacillariophyceae): life stages at the Weddell Sea ice edge, Phycologia, 29, 1, 27-38, 1990.

Gadd, PS, Heijnis, HH 2014, 'The potential of ITRAX core scanning: applications in quaternary science', Paper
1050   presented at the AQUA Biennial Meeting, The Grand Hotel, Mildura, 29th June - 4th July 2014.
Garrison, D. L. and Buck, K. R,: The biota of Antarctic pack ice in the Weddell Sea and Antarctic Peninsula regions, Polar Biology, 10, 3, 211-219, 1989.

Garrison, D. L., Buck, K. R, and Fryxell, G. A,: Algal assemblages in Antarctic pack ice and in ice-edge
1055   plankton 1, Journal of Phycology, 23, 4, 564-572, 1987.

Gersonde, R., Crosta, X., Abelmann, A. and Armand, L.: Sea-surface temperature and sea ice distribution of the Southern Ocean at the EPILOG Last Glacial Maximum-a circum-Antarctic view based on siliceous microfossil records, Quaternary Science Reviews, 24, 7, 869-896, 2005.
1060

Gersonde, R. and Zielinski, U.: The reconstruction of late Quaternary Antarctic sea-ice distribution- the use of diatoms as a proxy for sea-ice, Palaeogeography, Palaeoclimatology, Palaeoecology, 162, 3, 263-286, 2000.

Grobe, H. and Mackensen, A.: Late Quaternary climatic cycles as recorded in sediments from the Antarctic
1065   continental margin, The Antarctic paleoenvironment: A perspective on Global Change, Antarctic Research Series, 56, 349-376.

Hartman, J.D., Sangiorgi, F., Barcena, M.A., Tateo, F., Giglio, F., Albertazzi, S., Trincardi, F., Bijl, P.K., Langone, L. and Asioli, A.: Sea-ice, primary productivity and ocean temperatures at the Antarctic marginal zone
1070   during late Pleistocene. *Quaternary Science Reviews*, 266, 107069, 2021.

~~Harwood, D.M. and Maruyama, T.: Middle Eocene to Pleistocene diatom biostratigraphy of Southern Ocean sediments from the Kerguelen Plateau, LEG 120. *Wise, SW, Jr., Schlich, R., et al., Proc. ODP, Sci. Results*, 120, 683-733, 1992.~~

1075   Hemer, M., Post, A., O'Brien, P., Craven, M., Truswell, E., Roberts, D. and Harris, P.: Sedimentological signatures of the sub-Amery Ice Shelf circulation, Antarctic Science, 19, 4, 497, 2007.

Holder, L., Duffy, M., Opdyke, B., Leventer, A., Post, A., O'Brien, P. and Armand, L.K., 'Controls since the mid-Pleistocene transition on sedimentation and primary productivity downslope of Totten Glacier, East Antarctica' Paleoceanography and Paleoclimatology, 35, 12, p.e2020PA003981, 2021.

Hua, Q., Jacobsen, G. E., Zoppi, U., Lawson, E. M., Williams, A. A., Smith, A. M. and McGann, M. J.: Progress in radiocarbon target preparation at the ANTARES AMS Centre, Radiocarbon, 43, 2A, 275-282, 2001.

IBN 2020, 'IBN SPSS Statistics documentation' viewed 20th July 2020, https://www.ibm.com/docs/en/spss-statistics.

Ishikawa, A., Washiyama, N., Tanimura, A. and Fukuchi, M.: Variation in the diatom community under fast ice near Syowa Station, Antarctica, during the austral summer of 1997/98, Polar bioscience, 14, 10-23, 2001.

Jacobs, S. S.: On the nature and significance of the Antarctic Slope Front, Marine Chemistry, 35, 1-4, 9-24, 1991.

Johansen, J. R. and Fryxell, G. A.: The genus Thalassiosira (Bacillariophyceae): studies on species occurring south of the Antarctic Convergence Zone, Phycologia, 24, 2, 155-179, 1985.

Jouzel, J., Barkov, N., Barnola, J., Bender, M., Chappellaz, J., Genthon, C., Kotlyakov, V., Lipenkov, V., Lorius, C. and Petit, J.: Extending the Vostok ice-core record of paleoclimate to the penultimate glacial period, Nature, 364, 6436, 407-412, 1993.

Kaczmarska, I., Barbrick, N., Ehrman, J. and Cant, G.: Eucampia Index as an indicator of the Late Pleistocene oscillations of the winter sea-ice extent at the ODP Leg 119 Site 745B at the Kerguelen Plateau, Twelfth International Diatom Symposium, 103-112, 1993.

Kellogg, T. B. and Truesdale, R. S.: Late Quaternary paleoecology and paleoclimatology of the Ross Sea: the diatom record, Marine Micropaleontology, 4, 137-158, 1979.

Knox, G. A.: Biology of the southern ocean, 2nd Ed, *CRC Press Taylor and Francis Group, LCC, University of Canterbury, Christchurch*, 2006.

Kohfeld, K. E. and Chase, Z. : Temporal evolution of mechanisms controlling ocean carbon uptake during the last glacial cycle, Earth and Planetary Science Letters, 472, 206-215, 2017.

Kopczynska, E. E, Weber, L, and El-Sayed, S.: Phytoplankton species composition and abundance in the Indian sector of the Antarctic Ocean, Polar Biology, 6, 3, 161-169, 1986.

Kopczyńska, E. E., Fiala, M. and Jeandel, C.: Annual and interannual variability in phytoplankton at a permanent station off Kerguelen Islands, Southern Ocean, Polar Biology, 20, 5, 342-351, 1998.

Leventer, A.: Modern distribution of diatoms in sediments from the George V Coast, Antarctica, Marine Micropaleontology, 19, 4, 315-332, 1992.

Leventer, A., Domack, E., Dunbar, R., Pike, J., Stickley, C., Maddison, E., Brachfeld, S., Manley, P. and McClennen, C.: Marine sediment record from the East Antarctic margin reveals dynamics of ice sheet recession, GSA Today, 16, 12, 4, 2006.

Li, Q., Xiao, W., Wang, R. and Chen, Z.: Diatom based reconstruction of climate evolution through the Last Glacial Maximum to Holocene in the Cosmonaut Sea, East Antarctica, Deep Sea Research Part II: Topical Studies in Oceanography, 194, 104960, 2021.

Ligowski, R.: Phytoplankton of the Olaf Prydz Bay (Indian Ocean, East Antarctica) in February 1969', Polish Polar Research, 21-32, 1983.

Ligowski, R., Godlewski, M. and Lukowski, A.: Sea ice diatoms and ice edge planktonic diatoms at the northern limit of the Weddell Sea pack ice, in Proceedings of the NIPR Symposium on Polar Biology, 5, 9-20, 1992.

1135

Lisiecki, L. E. and Raymo, M. E.: A Pliocene-Pleistocene stack of 57 globally distributed benthic δ18O records, Paleoceanography, 20, 1, 2005.

Lucchi, R. G. and Rebesco, M.: Glacial contourites on the Antarctic Peninsula margin: insight for
1140   palaeoenvironmental and palaeoclimatic conditions, Geological Society, London, Special Publications, 276, 1, 111-127, 2007.

Lucchi, R. G., Rebesco, M., Camerlenghi, A., Busetti, M., Tomadin, L., Villa, G., Persico, D., Morigi, C., Bonci, M. C. and Giorgetti, G.: Mid-late Pleistocene glacimarine sedimentary processes of a high-latitude, deep-
1145   sea sediment drift (Antarctic Peninsula Pacific margin), Marine geology, 189, 3-4, 343-370, 2002.

Maddison, E. J., Pike, J. and Dunbar, R.: Seasonally laminated diatom-rich sediments from Dumont d'Urville Trough, East Antarctic margin: Late-Holocene neoglacial sea-ice conditions, The Holocene, 22, 8, 857-875, 2012.
1150

Maddison, E. J., Pike, J., Leventer, A., Dunbar, R., Brachfeld, S., Domack, E. W., Manley, P. and McClennen, C.: Post-glacial seasonal diatom record of the Mertz Glacier Polynya, East Antarctica, Marine Micropaleontology, 60, 1, 66-88, 2006.

1155   Martin, J. H., Fitzwater, S. E. and Gordon, R. M.: Iron deficiency limits phytoplankton growth in Antarctic waters, Global Biogeochemical Cycles, 4, 1, 5-12, 1990.
Massom, R. A., Scambos, T.A., Bennetts, L. G., Reid, P., Squire, V. A. and Stammerjohn, S. E.: Antarctic ice shelf disintegration triggered by sea ice loss and ocean swell, Nature, 558, 7710, 383-389, 2018.

1160   Masson-Delmotte, V., Schulz, M., Abe-Ouchi, A., Beer, J., Ganopolski, A., González Rouco, J. F., Jansen, E., Lambeck, K., Luterbacher, J., Naish, T., Osborn, T., Otto-Bliesner, B., Quinn, T., Ramesh, R., Rojas, M., Shao X. and Timmermann A.: Information from Paleoclimate Archives, 2013.

McMinn, A.: Late Holocene increase in sea ice extent in fjords of the Vestfold Hills, eastern Antarctica,
1165   Antarctic Science 12, 1, 80-88, 2000.

McMinn, A., Heijnisj, H., Harle, K. and McOrist, G.: Late-Holocene climatic change recorded in sediment cores from Ellis Fjord, eastern Antarctica, The Holocene, 11, 3, 291-300, 2001.

1170   Medlin, L. K. and Priddle, J.: Polar marine diatoms, British Antarctic Survey, 1990.

Minowa, M., Sugiyama, S., Ito, M., Yamane, S. and Aoki, S.: Thermohaline structure and circulation beneath the Langhovde Glacier ice shelf in East Antarctica, *Nature Communications*, 12, 1, 1-9, 2021.

1175   Minzoni, R.T., Anderson, J.B., Fernandez, R. and Wellner, J.S.: Marine record of Holocene climate, ocean, and cryosphere interactions: Herbert sound, James Ross Island, Antarctica, Quaternary Science Reviews, 129, 239-259, 2015.

Moisan, T. and Fryxell, G.: The distribution of Antarctic diatoms in the Weddell Sea during austral winter,
1180   Botanica Marina, 36, 6, 489-498, 1993.

Mortlock, R. A. and Froelich, P.N.: A simple method for the rapid determination of biogenic opal in pelagic marine sediments, Deep Sea Research Part A. Oceanographic Research Papers, 36, 9, 1415-1426, 1989.

Orsi, A. H., Whitworth III, T., and Nowlin Jr, W.D.: On the meridional extent and fronts of the Antarctic
1185   Circumpolar Current, *Deep Sea Research Part I: Oceanographic Research Papers* 42, 5, 641-673, 1995.

Passchier, S.: Linkages between East Antarctic Ice Sheet extent and Southern Ocean temperatures based on a Pliocene high-resolution record of ice-rafted debris off Prydz Bay, East Antarctica, Paleoceanography, 26, 4, 2011.

1190

Panizzo, V., Crespin, J., Crosta, X., Shemesh, A., Massé, G., Yam, R., Mattielli, N. and Cardinal, D.: Sea ice diatom contributions to Holocene nutrient utilization in East Antarctica, Paleoceanography, 29, 4, 328-343, 2014.

1195 Patterson, M.O., McKay, R., Naish, T., Escutia, C., Jimenez-Espejo, F.J., Raymo, M.E., Meyers, S.R., Tauxe, L., Brinkhuis, H., Klaus, A., Fehr, A., Bendle, J.A.P., Bijl, P.K., Bohaty, S.M., Carr, S.A., Dunbar, R.B., Flores, J.A., Gonzalez, J.J., Hayden, T.G., Iwai, M., Katsuki, K., Kong, G.S., Nakai, M., Olney, M.P., Passchier, S., Pekar, S.F., Pross, J., Riesselman, C.R., Röhl, U., Sakai, T., Shrivastava, P.K., Stickley, C.E., Sugasaki, S., Tuo, S., van de Flierdt, T., Welsh, K., Williams, T. & Yamane, M.: Orbital forcing of the East Antarctic ice sheet
1200 during the Pliocene and Early Pleistocene, *Nature Geoscience*, 7, 11, 841-847, 2014.

Pesjak, L.: The variability of ocean circulation, productivity, and sea ice in the Adélie region, East Antarctica, over the last two glacial cycles, PhD thesis, University of Tasmania, https://doi.org/10.25959/100.00047523, 2022.

1205

Post, A., Galton-Fenzi, B., Riddle, M., Herraiz-Borreguero, L., O'Brien, P., Hemer, M., McMinn, A., Rasch, D. and Craven, M.: Modern sedimentation, circulation and life beneath the Amery Ice Shelf, East Antarctica, Continental Shelf Research, 74, 77-87, 2014.

1210 Presti, M., Barbara, L., Denis, D., Schmidt, S., De Santis, L. and Crosta, X.: Sediment delivery and depositional patterns off Adélie Land (East Antarctica) in relation to late Quaternary climatic cycles, Marine geology, 284, 1-4, 96-113, 2011.

Pichon, J. J., Bareille, G., Labracherie, M., Labeyrie, L. D., Baudrimont, A. and Turon, J. L.: Quantification of
1215 the biogenic silica dissolution in Southern Ocean sediments. Quaternary Research, 37, 3, 361-378, 1992.

Pritchard, H. D., Arthern, R. J., Vaughan, D. G. and Edwards, L. A.: Extensive dynamic thinning on the margins of the Greenland and Antarctic ice sheets, Nature, 461, 7266, 971-975, 2009.

1220 Pritchard, H., Ligtenberg, S.R., Fricker, H.A., Vaughan, D.G., van den Broeke, M.R. & Padman, L., Antarctic ice-sheet loss driven by basal melting of ice shelves, *Nature*, 484, 7395, 502-505, 2012.

Pudsey, C. J.: Grain size and diatom content of hemipelagic sediments at Site 697, ODP Leg 113: A record of Pliocene-Pleistocene climate, in Proc. Ocean Drill. Program Sci. Results, 113, 111-120, 1990.

1225 Pudsey, C. J.: Late Quaternary changes in Antarctic Bottom Water velocity inferred from sediment grain size in the northern Weddell Sea, Marine geology, 107, 1-2, 9-33, 1992.

Pudsey, C. J. and Camerlenghi, A.: 'Glacial–interglacial deposition on a sediment drift on the Pacific margin of the Antarctic Peninsula, Antarctic Science, 10, 3, 286-308, 1998.

1230

Pudsey, C. J., Barker, P. F. and Hamilton, N.: Weddell Sea abyssal sediments a record of Antarctic Bottom Water flow, Marine geology, 81, 1-4, 289-314, 1988.

Quilty, P. G., Kerry, K. R. and Marchant, H. J.: A seasonally recurrent patch of Antarctic planktonic
1235 diatoms, *Search (Sydney)*, 16, 1-2, 1985.

Rembauville, M., Blain, S., Armand, L., Queguiner, B. and Salter, I.: Export fluxes in a naturally iron-fertilized area of the Southern Ocean-Part 2: Importance of diatom resting spores and faecal pellets for export, Biogeosciences, 12, 11, 3171-3195, 2015.

Romero, O. E., Armand, L. K., Crosta, X. and Pichon, J. J.: The biogeography of major diatom taxa in Southern
1240 Ocean surface sediments: 3. Tropical/Subtropical species, Palaeogeography, Palaeoclimatology, Palaeoecology, 223, 1-2, 49-65, 2005.

Rothwell, R.G. & Croudace, I.W.: 'Twenty Years of XRF Core Scanning Marine Sediments: What Do Geochemical Proxies Tell Us?', 17,. 25-102, 2015.

Salabarnada, A., Escutia, C., Röhl, U., Nelson, C.H., McKay, R., Jiménez-Espejo, F.J., Bijl, P.K., Hartman, J.D., Strother, S.L. & Salzmann, U.: Paleoceanography and ice sheet variability offshore Wilkes Land, Antarctica–Part 1: Insights from late Oligocene astronomically paced contourite sedimentation, *Climate of the Past*, 14, 7, 991-1014, 2018.

Schrader, H., Swanberg, I. L., Burckle, L. H. and Grønlien, L.: Diatoms in recent Atlantic (20 S to 70 N latitude) sediments: abundance patterns and what they mean, Twelwth International Diatom Symposium, 129-135, 1993.

Scott, F. and Thomas, D.: Diatoms, Antarctic marine protists, Australian Biological Resources Study, Canberra, 13-201, 2005.

Shemesh, A., Burckle, L. and Froelich, P.: Dissolution and preservation of Antarctic diatoms and the effect on sediment thanatocoenoses, Quaternary Research, 31, 2, 288-308, 1989.

Shi, G. R.: Multivariate data analysis in palaeoecology and palaeobiogeography—a review, Palaeogeography, Palaeoclimatology, Palaeoecology, 105, 3-4, 199-234, 1993.

Silvano, A., Rintoul, S. R., Peña-Molino, B., Hobbs, W. R., van Wijk, E., Aoki, S., Tamura, T. and Williams, G. D.: Freshening by glacial meltwater enhances melting of ice shelves and reduces formation of Antarctic Bottom Water, Science Advances, 4, 4, 2018.

Smetacek, V., Scharek, R., Gordon, L. I., Eicken, H., Fahrbach, E., Rohardt, G. and Moore, S.: Early spring phytoplankton blooms in ice platelet layers of the southern Weddell Sea, Antarctica, Deep Sea Research Part A. Oceanographic Research Papers, 39, 2, 153-168, 1992.

Smith, J. A., Hillenbrand, C. D., Pudsey, C. J., Allen, C. S. and Graham, A. G.: The presence of polynyas in the Weddell Sea during the Last Glacial Period with implications for the reconstruction of sea-ice limits and ice sheet history, Earth and Planetary Science Letters, 296, 3, 287-298, 2010.

Smith, W. O. and Nelson, D. M.: Importance of ice edge phytoplankton production in the Southern Ocean, BioScience, 36, 4, 251-257, 1986.
Spellerberg, I. F. and Fedor, P. J.: "A tribute to Claude Shannon (1916–2001) and a plea for more rigorous use of species richness, species diversity and the 'Shannon–Wiener' Index." *Global ecology and biogeography,* 12, 3,177-179, 2003.

Spreen, G., Kaleschke, L. and Heygster, G.: Sea ice remote sensing using AMSR-E 89-GHz channels, Journal of Geophysical Research: Oceans, 113, C2, 2008.

Stuiver, M. and Polach, H. A.: Discussion reporting of 14 C data, Radiocarbon, 19, 03, 355-363, 1977.

Tanimura, Y., Fukuchi, M., Watanabe, K. and Moriwaki, K.: Diatoms in water column and sea-ice in Lützow-Holm Bay, Antarctica, and their preservation in the underlying sediments, Bulletin of the National Science Museum, C, 16, 1, 15-39, 1990.

Taylor, F., McMinn, A., and Franklin, D.: Distribution of diatoms in surface sediments of Prydz Bay, Antarctica, Marine Micropaleontology, 32,3-4, 209-229, 1997.

Taylor, F. and McMinn, A.: Evidence from diatoms for Holocene climate fluctuation along the East Antarctic margin, The Holocene, 11, 4, 455-466, 2001.

Taylor, F., Whitehead, J. and Domack, E.: Holocene paleoclimate change in the Antarctic Peninsula: evidence from the diatom, sedimentary and geochemical record, Marine Micropaleontology, 41, 1-2, 25-43, 2001.

Tolotti, R., Salvi, C., Salvi, G. and Bonci, M.C., Late Quaternary climate variability as recorded by micropaleontological diatom data and geochemical data in the western Ross Sea, Antarctica, Antarctic Science, 25, 6, 804-820, 2013.

Tooze, S., Halpin, J.A., Noble, T.L., Chase, Z., O'Brien, P.E. and Armand, L.: Scratching the surface: A marine sediment provenance record from the continental slope of central Wilkes Land, East Antarctica, *Geochemistry, Geophysics, Geosystems* 21, 11, e2020GC009156, 2020.

1305 Truesdale, R. S. and Kellogg, T. B.: Ross Sea diatoms: modern assemblage distributions and their relationship to ecologic, oceanographic, and sedimentary conditions, Marine Micropaleontology, 4, 13-31, 1979.

Williams, G., Aoki, S., Jacobs, S., Rintoul, S., Tamura, T. and Bindoff, N.: Antarctic bottom water from the
1310 Adélie and George V Land coast, East Antarctica (140–149 E), Journal of Geophysical Research: Oceans, 115, C4, 2010.

Williams, G., Bindoff, N., Marsland, S. and Rintoul, S.: Formation and export of dense shelf water from the Adélie Depression, East Antarctica, Journal of Geophysical Research: Oceans, 113, C4, 2008.
1315
Williams, G., Herraiz-Borreguero, L., Roquet, F., Tamura, T., Ohshima, K., Fukamachi, Y., Fraser, A., Gao, L., Chen, H. and McMahon, C. The suppression of Antarctic bottom water formation by melting ice shelves in Prydz Bay, Nature Communications, 7, 12577, 2016.

1320 Williams, M.: RV Tangaroa Voyage Report Tan1302- Mertz Polynya Voyage 1 February to 14 March 2013, *NIWA, Wellington, New Zealand,* 19-33, 80, 2013.

Wilson, DJ, Bertram, RA, Needham, EF, van de Flierdt, T, Welsh, KJ, McKay, RM, Mazumder, A, Riesselman, CR, Jimenez-Espejo, FJ & Escutia, C, 'Ice loss from the East Antarctic Ice Sheet during late Pleistocene
1325 interglacials', *Nature*, vol. 561, no. 7723, p. 383, 2018.

Wu, L., Wang, R., Xiao, W., Ge, S., Chen, Z. and Krijgsman, W.: Productivity-climate coupling recorded in Pleistocene sediments off Prydz Bay (East Antarctica), Palaeogeography, Palaeoclimatology, Palaeoecology, 485, 260-270, 2017.
1330
Zielinski, U. and Gersonde, R.: Diatom distribution in Southern Ocean surface sediments (Atlantic sector): Implications for paleoenvironmental reconstructions, Palaeogeography, Palaeoclimatology, Palaeoecology, 129, 3-4, 213-250, 1997.

1335 Zielinski, U. and Gersonde, R.: Plio–Pleistocene diatom biostratigraphy from ODP Leg 177, Atlantic sector of the Southern Ocean. *Marine Micropaleontology*, 45, 3-4, 225-268, 2002.

Supplement of

Sea ice and productivity changes over the last glacial cycle in the Adélie Land region, East Antarctica, based on diatom assemblage variability

Lea Pesjak et al. ~~2021~~2023

Correspondence to Lea Pesjak (lea.pesjak@utas.edu.au)

Table S1 Environmental interpretation of diatom species identified within Tan_44, based on water column and sediment studies from coastal Antarctica to Subantarctic Southern Ocean. The three species types identified by both types of studies include: sea ice associated species (blue), open ocean associated species (yellow), and warmer water associated species (orange; Medlin and Priddle 1990). This list includes *Eucampia* ~~antarctica~~ index (Terminal/ Intercalary valve ratio). This list suggests there are some differences in interpretation of species habitat depending on the type of study conducted. Reference notes are: 1) Medlin and Priddle (1990); 2) Ligowski, Godlewski and Lukowski (1992); 3) Garrison and Buck (1989); 4) Kopczynska, Weber and El-Sayed (1986); 5) Tanimura et al. (1990); 6) Scott and Thomas (2005); 7) Kopczyńska, Fiala and Jeandel (1998); 8) Ligowski (1983); 9) Garrison, Buck and Fryxell (1987); 10) Beans et al. (2008); 11) Fryxell (1991); 12) Moisan and Fryxell (1993); 13) Doucette and Fryxell (1985); 14) Johansen and Fryxell (1985); 15) Smetacek et al. (1992); 16) Bodungen et al. (1986); 17) Smith and Nelson (1986); 18) Ishikawa et al. (2001); 19) Pichon et al. (1992); 20) Armand et al. (2005); 21) Romero et al. (2005); 22) Zielinski and Gersonde (1997); 23) Kaczmarska et al. (1993); 24) Leventer (1992); 25) Taylor, McMinn and Franklin (1997); 26) Crosta et al. (2005).

ENVIRONMENTAL INTERPRETATION

W	S	Species/ index	WATER COLUMN AND SEA ICE STUDIES	SEDIMENT SURFACE STUDIES
op	si	*Actinocyclus actinochilus* (Ehrenberg) Simonsen	Sea ice edge; rare in ice; coastal [1,2,3]	Sea ice >7 months/yr; sea ice edge; along ice shelves [19,20]
op	w	*Azpeitia tabularis*	Subantarctic, rare near sea ice [1]	Open ocean, warmer water; north of Polar Front [21,22]
op	w	*Asteromphalus hyalinus* Karsten	Coastal, north and south of Polar Front [4,5,6]	Open ocean, warmer water; north of Polar Front [21]
op	w	*Asteromphalus parvulus* Karsten	Coastal; north and south of Polar Front [4,6]	Open ocean, warmer water; north of Polar Front [21]
op		*Chaetoceros bulbosum* (Ehrenberg) Heiden	Open ocean; south of Polar Front; rare in ice [7,3]	
op		*Chaetoceros dichaeta* (Ehrenberg)	Open ocean; sea ice; south of Polar Front [8,9,4,7]	
op	op	*Eucampia antarctica* (Castracane) Mangin	Open ocean; south of Polar Front; rare in sea ice [3,10]	Coastal to Subtropical Front; increases in glacial intervals [22,23]
si	si	*Eucampia* index	Higher index indicates Winter stage (Prydz Bay) i.e. more sea ice [11]	Sea ice; along ice shelves (Ross Sea) [19,23]
op	op	*Fragilariopsis kerguelensis*	Open ocean; south of Polar Front; rare in sea ice; increases offshore [4,3,7]	Open ocean; increases seaward; winter sea ice edge; Polar Front [20,22,24]
op	si	*Fragilariopsis angulata*	Open ocean [1]	Sea ice; coastal [25]
si	si	*Fragilariopsis cylindrus*	Sea ice; sea ice edge; open ocean; coastal; winter sea ice edge [9,12,2]	Sea ice >7 months/yr; coastal [20,22]
si	si	*Fragilariopsis linearis*	Sea ice; ice edge [1,12]	Sea ice; along ice shelves [19,20]
si	si	*Fragilariopsis obliquecostata*	Sea ice [3]	Sea ice >7 months/ yr; sea ice edge [20]
si	si	*Fragilariopsis sublinearis*	Sea ice; sea ice edge [1,12]	Sea ice >7 months/ yr [19,20]
op	op	*Rhizosolenia antennata*	Open ocean [10]	Open ocean; cooler water; sea ice edge [26]
op	op	*Rhizosolenia styliformis* Brightwell	Open ocean; south of 62°S/ south of Polar Front; rare in sea ice [4,3]	Open ocean; cooler water; sea ice edge [26]
si	si	*Stellarima microtrias* (Ehrenberg) Hasle & Sims	Sea ice; cold waters [6]	Sea ice [20]
op	op	*Thalassiosira lentiginosa* (Janish) Fryxell	Open ocean; south of the Polar Front [14]	Open ocean; 0-7°C; between winter sea ice edge and Polar Front; coastal [26,22,25]
op	op	*Thalassiosira oliverana*	Open ocean; antarctic and subantarctic [1]	Open ocean; between winter sea ice edge to Polar Front [26]
op	si	*Thalassiosira tumida* (Janish) Hasle	Open ocean; ice edge; sea ice; coastal; common south of Polar Front [3,17,18,14]	Sea ice >8.5 months/yr [20]
op	op	*Thalassiothrix antarctica*	Open ocean; coastal; sea ice edge; south of Polar Front [2,10,8,7]	Open ocean; diatom ooze belt [19,26]
op	op	*Thalassiothrix longissima* Cleve and Grunow	Open ocean; rare in sea ice [3]	Open ocean [26]
op	op	*Trichotoxon reinboldii*	Open ocean [1]	Open ocean; cooler water; south of Polar Front [26,25]

W   interpretation based on water column studies

S   interpretation based on sediment surface studies

si   sea ice related species
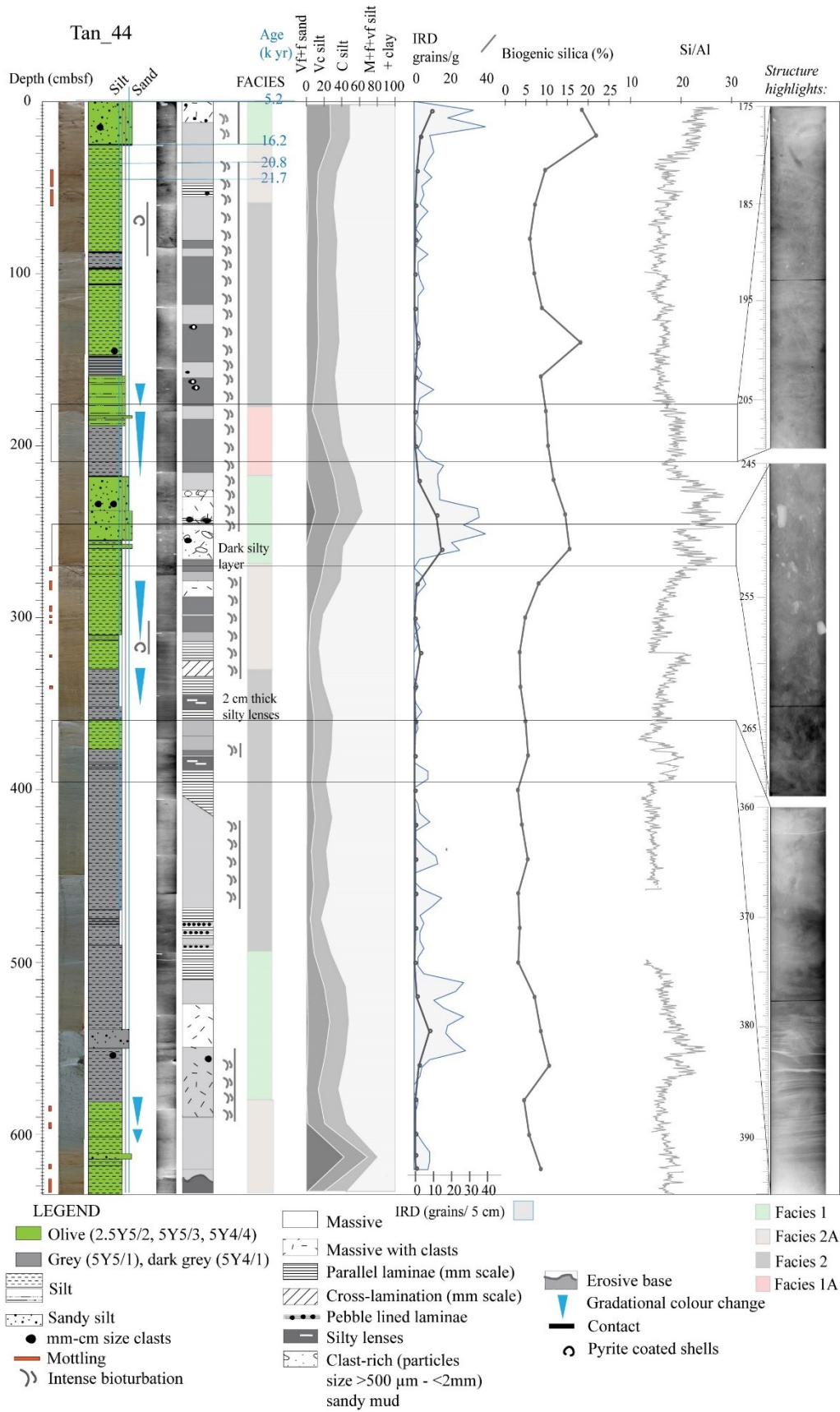
Figure S1 Lithology, structure, grain size, biogenic silica, ice rafted debris (IRD) counted from sieved sections (grains/g) and from X-radiographs (grains/ 5 cm), Si/Al (XRF-derived~~)), and diatom and radiolaria estimates of the sand fraction (symbols)~~. Included in this figure is the facies interpretation of core Tan_44. The facies model

is based upon primary lithology identified in core logs (olive sandy mud; olive mud; grey mud; and olive-grey mud), Si/Al, biogenic silica and IRD results. Included are X-radiographs of parts of core.

S1 Development of ~~the~~ facies model

S1.1 Methods

Tan_44 lithology was described on the voyage (Williams 2013). The X-radiographs were completed at the National Institute of Water and Atmospheric Research (NIWA; Williams 2013). ~~Sampling for grain size, biogenic silica, and ice rafted debris (IRD) were taken at 20 cm resolution down core. Sampling for diatom analysis were taken at 10 cm resolution within 350–0 cm interval. Microfossil and micropyrite estimates were completed using a binocular microscope, on a sieved sand (>63 μm) fraction.~~

S1.1.1 Grain Size

Grain size was determined using a Beckman Coulter 13320 laser diffraction particle size analyser. Sampling for grain size was taken at 20 cm resolution down core. A sample size of 0.5 x 0.5 cm was soaked overnight in a mixture of sodium hydrogen carbonate, sodium carbonate (anhydrous) and water. The sediment in solution was then shaken and placed through a sonic bath for 10 second intervals, several times, to disaggregate clay. This sample was poured into the grain size analyser through a 1.8 mm sieve and analysed for 60 seconds, prior to a 3-minute cleaning routine. The grain size statistics were calculated using GradistatV8 software (Blott & Pye 2001), which uses the Folk and Ward method for size distribution and description.

S1.1.2 ~~Ice Rafted Debris (IRD)~~

~~Ice rafted debris (IRD) analysis was completed using two methods, counting visible grains from X-radiographs (grains ≥1 mm, in 5 cm sections), and counting sieved grains (grains >500 μm; and dividing the number by weight, g). The size >500 μm, medium sand (Patterson et al. 2014) was chosen as the size that defines IRD because laser particle diffraction of samples showed the grain size <250 μm forms the matrix of all the samples. This is in contrast to other Antarctic studies, which defined IRD as >2 mm (Grobe et al. 1992; Diekmann et al. 2003), very coarse sand size, >1 mm , >250 μm , and >125 μm .~~

~~S1.1.3~~ X-ray fluorescence (XRF) data: Fe, Ti, Fe/Ti, Ba/Ti, Zr/Rb

The XRF methods are explained in ~~main text~~the manuscript under section Si/Al.

S1.2 Results

S1.2.1 Lithology

Four lithological units are identified in Tan_44 (Fig. S1), based on visual logs (Williams 2013) and structural features identified in X-radiographs (Fig. S1). Unit 1 is olive sandy mud, comprising olive (2.5Y5/2, 5Y5/3), or grey colour (5Y4/1, 5Y5/1) within 581-493 cm section, and is characterised by a sandy texture, massive structure with dispersed >1 mm sized grains. Unit 2A is olive mud (2.5Y5/2; 5Y4/4) comprising a massive structure, bioturbation, and rare traction structures, i.e., lenses and laminae. Mottling is found at 46-37 cm; 58-54 cm; 584 cm, 594 cm, and 619 cm. Unit 2 is grey mud, comprising grey (5Y5/1) and olive (2.5Y5/2) colour, within section 147-59 cm and is characterised by a finer texture (than Unit 1). The younger Unit 2 (178-59 cm) contains a massive structure with evident bioturbation within the 147-59 cm section, while the older Unit 2 (493-331 cm) contains laminae and pebble-lined laminae. Gradation is observed at the base of the younger unit (at 178-159 cm), and within the lower unit (at 353-331 cm). Unit 1A is olive-grey mud (2.5Y 5/2) comprising a finer texture (than in Unit 1), with a massive structure and evident bioturbation.

~~Diatom and radiolaria species percentage were estimated for the sand fraction. The diatom estimates range from 0 - ~20%, while the radiolaria estimates range from 0 - ~97%, per sand fraction of the sample (Fig. S1). This interpretation is dependent on the total amount of the sand fraction per sample and is therefore only an estimate of surface productivity. Intervals with highest diatom estimates (5-10%) are found in olive sandy mud (Unit 1). Intervals with highest radiolaria estimates (20-80%) coincide with 280-0 cm (Unit 1; 1A; 2; 2A), and 620-520 cm (Unit 1, 2A) sections. Pyrite coated foraminifera and radiolaria shells, and some framboidal pyrite are found at 80-60 cm (Unit 2A), and at 320-300 cm (Unit 2A; Fig. S1).~~

~~**S1.2.1**~~**S1.2.2** **Grain size**

A down core grain size pattern exists, formed by the alternation of coarser grained (sandy silt) and finer grained (silt) sediments (Fig. S1). The sandy silt intervals consist of 1-9% very fine to fine sand and, 19-27% very coarse silt. The silt intervals consist of increased medium silt to clay, up to 68% in the upper core, and up to 86% in the lower core. The sandy silt intervals coincide with higher Zr/Rb values and Unit 1. The silt intervals coincide with lower Zr/Rb, and Unit 2, Unit 2A and Unit 1A (Fig S1; Fig. S2).

~~**S1.2.2 Ice rafted debris**~~

~~High counts of ice rafted debris (IRD; 4-36 grains/5 cm) are found in Unit 1 (Fig. S1), with maximum counts found at 15-10 cm, at 255-250 cm and at 500-495 cm. Lower numbers of IRD (0-14 grains/5 cm) are found in Unit 2, Unit 2A and Unit 1A.~~

S1.2.3 X-ray fluorescence (XRF) data: Fe, Ti, Fe/Ti, Ba/Ti, Zr/Rb

Fe and Ti are generally parallel down core. Fe values range from ~23,000- ~44,000 counts per second (cps) and Ti values range from ~ 6,000-25,000 cps. Lower Fe values (~<33,000) are found in core sections 30-0 cm, 280-220 and 575-500 cm, which coincide with Unit 1 (Fig. S2). Similarly, lower Ti values occur in Unit 1. Fe/Ti values range from ~1.3- ~2.0, with lower values (<1.5) at 30-0 cm, 285-218 cm, and 580-500 cm, coinciding with Unit 1, and higher values (>1.5) coinciding with Unit 2 and Unit 2A.

Ba/Ti and Zr/Rb are generally parallel down core, aligned with Si/Al (Fig. S2), except within 255-230 cm (Unit 1) section where Ba/Ti decreases significantly. Ba/Ti values range from 0-0.06, with highest values (0-0.06) associated with Unit 1 and Unit 1A, and lower values (0-0.04) associated with Unit 2 and Unit 2A, and in the 255-230 cm section of Unit 1. Zr/Rb values range from 0.6-1.8, with highest values (~>1) associated with Unit 1 and Unit 1A, and lower values (~<1) associated with Unit 2 and Unit 2A, except in 331-328 cm section of Unit 2A, where slightly higher Zr/Rb values are found.
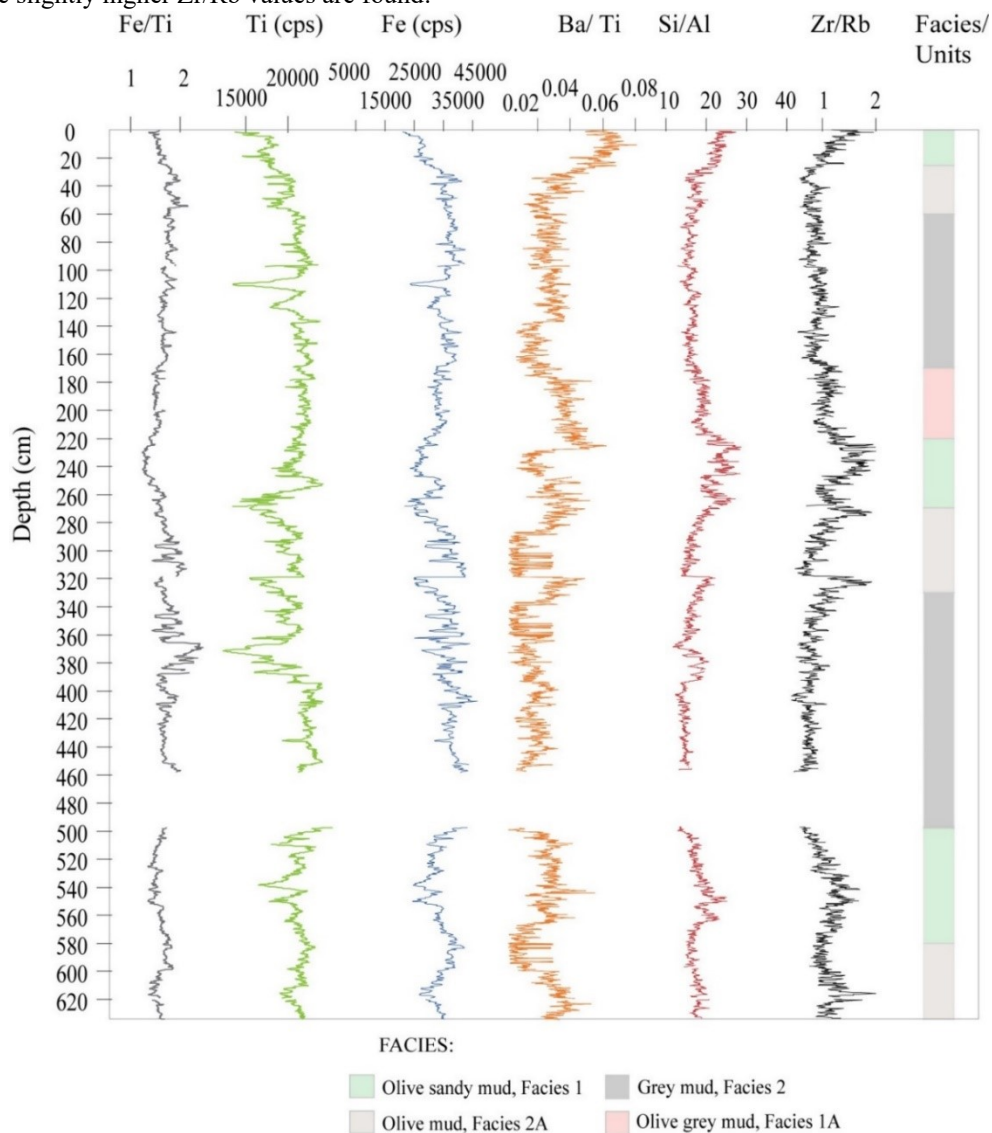
Figure S2 XRF data in Tan_44: Fe/Ti; Fe; Ti; Ba/Ti; Si/Al and Zr/Rb down core values, compared to glacial, interglacial, deglacial and glaciation facies occurrence.

Table S2 Q-mode principal component factor loadings of each principal component (assemblage; PC 1-~~4~~3).

	PC 1	PC 2	PC 3
Fragilariopsis kerguelensis	0.258	0.081	-0.282
Actinocyclus actinochilus	-0.636	-0.146	0.628
Eucampia antarctica	-0.935	-0.209	0.000
Fragilariopsis group	-0.200	0.904	-0.039
Actinocyclus ingens	-0.074	-0.218	0.801
Thalassiosira tumida	0.179	0.566	0.010
Thalassiosira oestrupii	0.283	-0.007	0.029
Asteromphalus parvulus	0.068	0.669	-0.093
Astermophalus hyalinus	0.480	0.257	-0.256
Thalassiosira lentiginosa	0.983	0.100	-0.118
Azpeitia tabularis	0.675	-0.296	-0.048
Thalassiosira oliverana	0.030	0.328	0.525

Table ~~S4~~S3 R-mode principal factor analysis: the main components (PC 1-~~4~~2) loadings down core.

Depth (cm)	PC 1	PC 2
10	0.961	0.262
20	0.946	0.297
30	0.973	0.222
40	0.964	0.121
50	0.972	0.132
60	0.635	0.682
70	0.119	0.990
80	0.185	0.981
90	0.113	0.988
100	0.157	0.982
110	0.470	0.881
120	0.328	0.943
130	0.566	0.816
140	0.506	0.858
150	0.872	0.481
160	0.760	0.639
170	0.621	0.752
180	0.804	0.546
190	0.797	0.592
200	0.803	0.565
210	0.489	0.741
220	0.831	0.329
230	0.939	0.334
240	0.867	0.469
250	0.873	0.477
260	0.940	0.330
270	0.974	0.168
280	0.662	0.740
290	0.672	0.735

Table S5S4 List of diatom species in Tan_44, including terminal and intercalary valve counts of *Eucampia antarctica*.

DEPTH (cm)	5	20	30	40	50	60	70	80	90	100	110	120
Actinocyclus actinochilus	7	12	12	20	9	51	28	15	75	27	39	46
Actinocyclus ingens	1	1				45	7		4	2	2	4
Asteromphalus hookeri	5	5	3	6	8		1	3	1	2	1	1
Asteromphalus hyalinus	2	5	5	5	4		2					
Asteromphalus parvulus	4	3	3		3			1		3	1	1
Azpeitia tabularis	14	24	22	31	31				4	1	4	4
Chaetoceros bulbosum				10								
Chaetoceros chriophilus												
Chaetoceros adelianum				1								
Chaetoceros dichaeta												
Chaetoceros flexuosus												
Cocconeis costata												
Coscinodiscus asteromphalus		2									2	
Coscinodiscus bouvet				1		1						
Coscinodiscus curvatulus	1	6		2	5							
Coscinodiscus oculoides			1	1			1		1			1
Coscinodiscus radiatus				1					1			
Coscinodiscus marginatus												
Coscinodiscus vulnificus		1						1	1			
Eucampia antarctica terminal valve	3	13	9	3	7	41	108	43	100	120	59	103
Eucampia antarctica intercalary valve	30	25	13	7	5	61	140	82	226	222	120	127
Eucampia antarctica	33	38	22	10	12	102	248	125	326	342	179	230
Fragilariopsis kerguelensis	42	8	27	83	87		4		12	13	6	9
Fragilariopsis obliquecostata	1								2		3	1
Fragilariopsis sublinearis	1	1									1	2
Fragilariopsis linearis												
Fragilariopsis rhombica												
Fragilariopsis cylindrus												
Fragilariopsis curta												
Fragilariopsis vanheurckii												
Fragilariopsis seriata	1											
Fragilariopsis ritscherii									1			
Fragilariopsis barbieri					1							
Fragilariopsis pseudonana					1							
Porosira glacialis	2			1		1	1	2			1	
Porosira pseudodenticulata							2					
Rhizosolenia styliformis				1				2		1		
Rhizosolenia polydactyla												
Rhizosolenia sp.							1	1	1			
Rhizosolenia hebetata												
Rhizosolenia setigera							1					
Rhizosolenia antennata												
Rhizosolenia (twin process) antennata												1
Proboscia inermis												
Rhizosolenia curvata												
Stellarima microtrias	3	2	1	1	0	6	1	0	8	5	7	3
Thalassiosira gracilis	2	1		1		1	3	1			4	
Thalassiosira lentiginosa	291	307	324	266	319	164	87	53	118	130	157	144
Thalassiosira oestrupii		2	9	13	12	1	2	2	3	1	3	1
Thalassiosira oliveriana	25	24	9	6	12	26	9	4	17	15	10	17
Thalassiosira ritscherii	2				1	1						
Thalassiosira tumida	5	3	4	9	4		1	2	2	3	3	7
Thalassiothrix antarctica		2		11					1			
Thalassiothrix longisima	1				3							
Trichotoxon reinboldii			1	2	1							
Triceratium spp.												
Total counts	444	446	443	482	513	399	399	212	578	545	423	472

DEPTH (cm)	130	140	150	160	170	180	190	200	210	220	230	240
Actinocyclus actinochilus	46	37	26	29	32	17	24	35	29	20	19	31
Actinocyclus ingens	2	1	1							1		1
Asteromphalus hookeri	2	6	1	8	7	1		2			3	1
Asteromphalus hyalinus		3	16	7	11	1	7	4	3	1	4	9
Asteromphalus parvulus	4	4	1	6	10	6		10	2	2	6	6
Azpeitia tabularis	5		1	3			1	5	4	3	9	4
Chaetoceros bulbosum					4	1						1
Chaetoceros chriophilus					1			1				
Chaetoceros adelianum												
Chaetoceros dichaeta		2						20				
Chaetoceros flexuosus				2			1	4				
Cocconeis costata												2
Coscinodiscus asteromphalus						1					1	1
Coscinodiscus bouvet												
Coscinodiscus curvatulus				2	2	1	1	1				2
Coscinodiscus oculoides		3			1	3			1			
Coscinodiscus radiatus												
Coscinodiscus marginatus										1		
Coscinodiscus vulnificus				1				1				
Eucampia antarctica terminal valve	42	58	20	19	35	8	22	20	35	14	11	17
Eucampia antarctica intercalary valve	102	111	65	104	125	73	92	73	163	32	34	79
Eucampia antarctica	144	169	85	123	160	81	114	93	198	46	45	96
Fragilariopsis kerguelensis	11		24	35	58	46	23	42	126	92	15	8
Fragilariopsis obliquecostata	2	1		26	28	31	31	32	7	6	3	5
Fragilariopsis sublinearis	2							1	3			
Fragilariopsis linearis										3		
Fragilariopsis rhombica										2	1	
Fragilariopsis cylindrus												
Fragilariopsis curta												
Fragilariopsis vanheurckii												
Fragilariopsis seriata												
Fragilariopsis ritscherii												
Fragilariopsis barbieri												
Fragilariopsis pseudonana												
Porosira glacialis	1	1	1		1			2				
Porosira pseudodenticulata												
Rhizosolenia styliformis	3	5	3	5	5	4	7	7	2	2	1	2
Rhizosolenia polydactyla					1						1	
Rhizosolenia sp.		2										
Rhizosolenia hebetata					1							
Rhizosolenia setigera												
Rhizosolenia antennata					1							
Rhizosolenia (twin process) antennata				1	2			1	2	1	1	
Proboscia inermis								1				
Rhizosolenia curvata		1										
Stellarima microtrias	5	2	3	3	6	5	6	3	0	0	0	1
Thalassiosira gracilis	2		3								1	4
Thalassiosira lentiginosa	162	164	284	227	194	180	249	202	179	165	293	325
Thalassiosira oestrupii	6	8		8	3	3	6	2	4	3	3	14
Thalassiosira oliveriana	10	11	16	9	16	11	23	26	22	5	19	47
Thalassiosira ritscherii							1	4	1		1	
Thalassiosira tumida	7	1	3	12	11	5	10	12	3	3	10	23
Thalassiothrix antarctica												
Thalassiothrix longisima												
Trichotoxon reinboldii												
Triceratium spp												
Total counts	414	421	468	507	555	397	504	510	587	356	436	583

DEPTH (cm)	250	260	270	280	290	300	310	320	330	340	350
Actinocyclus actinochilus	15	34	3	31	37	5	9	1	1		
Actinocyclus ingens	1			13	7		12				
Asteromphalus hookeri	7	3	1	4	3		2				
Asteromphalus hyalinus	10	5	9	1	1		2				
Asteromphalus parvulus	2	1	3		1						
Azpeitia tabularis	20	27		2			1				
Chaetoceros bulbosum											
Chaetoceros chriophilus											
Chaetoceros adelianum											
Chaetoceros dichaeta											
Chaetoceros flexuosus											
Cocconeis costata	1										
Coscinodiscus asteromphalus		1		1			1				
Coscinodiscus bouvet											
Coscinodiscus curvatulus	1	8	1	1						1	1
Coscinodiscus oculoides	1				2						
Coscinodiscus radiatus				1	2						
Coscinodiscus marginatus					2		2			1	
Coscinodiscus vulnificus											
Eucampia antarctica terminal valve		7	2		21	9	4	1			2
Eucampia antarctica intercalary valve	87	71	11	137	118	37	61	3	2	1	2
Eucampia antarctica	87	78	13	137	139	46	65	4	2	1	4
Fragilariopsis kerguelensis	9	63	74	28	8		10				
Fragilariopsis obliquecostata			1	3	4						
Fragilariopsis sublinearis				6	2						
Fragilariopsis linearis		2		2							
Fragilariopsis rhombica											
Fragilariopsis cylindrus			3		5						
Fragilariopsis curta							1				
Fragilariopsis vanheurckii							1				
Fragilariopsis seriata											
Fragilariopsis ritscherii											
Fragilariopsis barbieri											
Fragilariopsis pseudonana											
Porosira glacialis				1							
Porosira pseudodenticulata											
Rhizosolenia styliformis				2	2		1				
Rhizosolenia polydactyla											
Rhizosolenia sp.											
Rhizosolenia hebetata											
Rhizosolenia setigera				2	2	2					
Rhizosolenia antennata											
Rhizosolenia (twin process) antennata											
Proboscia inermis		1									
Rhizosolenia curvata											
Stellarima microtrias	2	5	16	5	2	2	1	0	0	0	0
Thalassiosira gracilis	2	1			3	1					
Thalassiosira lentiginosa	292	481	358	191	208	28	122	5	11	1	2
Thalassiosira oestrupii	2	7	3	4	2	2	3		1		
Thalassiosira oliveriana	10	3	1	18	10	2	9	0	1	5	0
Thalassiosira ritscherii				1	1		2				
Thalassiosira tumida	11	10			4	1	4				
Thalassiothrix antarctica		3									
Thalassiothrix longisima		3									
Trichotoxon reinboldii		1									
Triceratium spp					1						1
Total counts	473	737	486	454	448	89	248	10	16	9	8

References

Blott, S. J. and Pye, K.: GRADISTAT: a grain size distribution and statistics package for the analysis of unconsolidated sediments, Earth surface processes and Landforms, 26, 11, 1237-1248, 2001.

Cook, C. P., van de Flierdt, T., Williams, T., Hemming, S. R., Iwai, M., Kobayashi, M., Jimenez Espejo, F. J., Escutia, C., González, J. J., Khim, B. K., McKay, R. M., Passchier, S., Bohaty, S. M., Riesselman, C. R., Tauxe, L., Sugisaki, S., Galindo, A. L., Patterson, M. O., Sangiorgi, F., Pierce, E. L., Brinkhuis, H., Klaus, A., Fehr, A., Bendle, J. A. P., Bijl, P. K., Carr, S. A., Dunbar, R. B., Flores, J. A., Hayden, T. G., Katsuki, K., Kong, G. S., Nakai, M., Olney, M. P., Pekar, S. F., Pross, J., Röhl, U., Sakai, T., Shrivastava, P. K., Stickley, C. E., Tuo, S., Welsh, K. and Yamane, M.: Dynamic behaviour of the East Antarctic ice sheet during Pliocene warmth, Nature Geoscience, 6, 765, 2013.

Diekmann, B., Fütterer, D., Grobe, H., Hillenbrand, C., Kuhn, G., Michels, K., Petschick, R. and Pirrung, M.: Terrigenous sediment supply in the polar to temperate South Atlantic: Land-ocean links of environmental changes during the late Quaternary, in The South Atlantic in the Late Quaternary, Springer, 375-399, 2003.

Grobe, H. and Mackensen, A.: Late Quaternary climatic cycles as recorded in sediments from the Antarctic continental margin, The Antarctic Paleoenvironment: A Perspective on Global Change: Part One, 349-376, 1992.

Lisiecki, L. E. and Raymo, M. E.: A Pliocene-Pleistocene stack of 57 globally distributed benthic $\delta18O$ records, Paleoceanography, 20, 1, 2005.

Passchier, S.: Linkages between East Antarctic Ice Sheet extent and Southern Ocean temperatures based on a Pliocene high-resolution record of ice-rafted debris off Prydz Bay, East Antarctica, Paleoceanography, 26, 4, 2011.

Patterson, M. O., McKay, R., Naish, T., Escutia, C., Jimenez-Espejo, F. J., Raymo, M. E., Meyers, S. R., Tauxe, L., Brinkhuis, H., Klaus, A., Fehr, A., Bendle, J. A. P., Bijl, P. K., Bohaty, S. M., Carr, S. A., Dunbar, R. B., Flores, J. A., Gonzalez, J. J., Hayden, T. G., Iwai, M., Katsuki, K., Kong, G. S., Nakai, M., Olney, M. P., Passchier, S., Pekar, S. F., Pross, J., Riesselman, C. R., Röhl, U., Sakai, T., Shrivastava, P. K., Stickley, C. E., Sugasaki, S., Tuo, S., van de Flierdt, T., Welsh, K., Williams, T. and Yamane, M.: Orbital forcing of the East Antarctic ice sheet during the Pliocene and Early Pleistocene, Nature Geoscience, 7, 11, 841-847, 2014.

Pudsey, C. J. and Camerlenghi, A.: 'Glacial-interglacial deposition on a sediment drift on the Pacific margin of the Antarctic Peninsula, Antarctic Science, 10, 3, 286-308, 1998.

Armand, L K., Crosta, X., Romero, O. and Pichon, J. J.: The biogeography of major diatom taxa in Southern Ocean sediments: 1. Sea ice related species, Palaeogeography, Palaeoclimatology, Palaeoecology, 223, 1-2, 93-126, 2005.

Beans, C., Hecq, J. H., Koubbi, P., Vallet, C., Wright, S. and Goffart, A.: A study of the diatom-dominated microplankton summer assemblages in coastal waters from Terre Adélie to the Mertz Glacier, East Antarctica (139 E-145 E), Polar Biology, 31, 9, 1101-1117, 2008.

Blott, S. J. and Pye, K.: GRADISTAT: a grain size distribution and statistics package for the analysis of unconsolidated sediments, Earth surface processes and Landforms, 26, 11, 1237-1248, 2001.

Bodungen, B. V., Smetacek, V. S., Tilzer, M. M. and Zeitzschel, B.: Primary production and sedimentation during spring in the Antarctic Peninsula region, Deep Sea Research Part A. Oceanographic Research Papers, 33, 2, 177-194, 1986.

Crosta, X., Romero, O., Armand, L. K. and Pichon, J. J.: The biogeography of major diatom taxa in Southern Ocean sediments: 2. Open ocean related species, Palaeogeography, Palaeoclimatology, Palaeoecology, 223, 1-2, 66-92, 2005.

Doucette, G. J. and Fryxell, G. A.: Thalassiosira antarctica (Bacillariophyceae): Vegetative and resting stage ultrastructure of an ice-related marine diatom, Polar Biology, 4, 2, 107-112, 1985.

Fryxell, G.: Comparison of winter and summer growth stages of the diatom Eucampia antarctica from the Kerguelen Plateau and south of the Antarctic convergence zone, Proc. ODP. Sci. Results, 119, 675-685, 1991.

Garrison, D. L., Buck, K. R, and Fryxell, G. A.: Algal assemblages in Antarctic pack ice and in ice-edge plankton 1, Journal of Phycology, 23, 4, 564-572, 1987.

Garrison, D.L. and Buck, K.R.: The biota of Antarctic pack ice in the Weddell Sea and Antarctic Peninsula regions. *Polar biology*, 10 (3), 211-219, 1989.

Ishikawa, A., Washiyama, N., Tanimura, A. and Fukuchi, M.: Variation in the diatom community under fast ice near Syowa Station, Antarctica, during the austral summer of 1997/98, Polar bioscience, 14, 10-23, 2001.

Kaczmarska, I., Barbrick, N., Ehrman, J. and Cant, G.: Eucampia Index as an indicator of the Late Pleistocene oscillations of the winter sea-ice extent at the ODP Leg 119 Site 745B at the Kerguelen Plateau, Twelfth International Diatom Symposium, 103-112, 1993.

Kopczynska, E. E, Weber, L, and El-Sayed, S.: Phytoplankton species composition and abundance in the Indian sector of the Antarctic Ocean, Polar Biology, 6, 3, 161-169, 1986.

Kopczyńska, E. E., Fiala, M. and Jeandel, C.: Annual and interannual variability in phytoplankton at a permanent station off Kerguelen Islands, Southern Ocean, Polar Biology, 20, 5, 342-351, 1998.

Johansen, J. R. and Fryxell, G. A.: The genus Thalassiosira (Bacillariophyceae): studies on species occurring south of the Antarctic Convergence Zone, Phycologia, 24, 2, 155-179, 1985.

Leventer, A.: Modern distribution of diatoms in sediments from the George V Coast, Antarctica, Marine Micropaleontology, 19, 4, 315-332, 1992.

Ligowski, R.: Phytoplankton of the Olaf Prydz Bay (Indian Ocean, East Antarctica) in February 1969', Polish Polar Research, 21-32, 1983.

Ligowski, R., Godlewski, M. and Lukowski, A.: Sea ice diatoms and ice edge planktonic diatoms at the northern limit of the Weddell Sea pack ice, in Proceedings of the NIPR Symposium on Polar Biology, 5, 9-20, 1992.

Medlin, L. K. and Priddle, J.: Polar marine diatoms, British Antarctic Survey, 1990.
Moisan, T. and Fryxell, G.: The distribution of Antarctic diatoms in the Weddell Sea during austral winter, Botanica Marina, 36, 6, 489-498, 1993.

Pichon, J. J., Bareille, G., Labracherie, M., Labeyrie, L. D., Baudrimont, A. and Turon, J. L.: Quantification of the biogenic silica dissolution in Southern Ocean sediments. Quaternary Research, 37, 3, 361-378, 1992.

Romero, O. E., Armand, L. K., Crosta, X. and Pichon, J. J.: The biogeography of major diatom taxa in Southern Ocean surface sediments: 3. Tropical/Subtropical species, Palaeogeography, Palaeoclimatology, Palaeoecology, 223, 1-2, 49-65, 2005.

Scott, F. and Thomas, D.: Diatoms, Antarctic marine protists, Australian Biological Resources Study, Canberra, 13-201, 2005.

Smetacek, V., Scharek, R., Gordon, L. I., Eicken, H., Fahrbach, E., Rohardt, G. and Moore, S.: Early spring phytoplankton blooms in ice platelet layers of the southern Weddell Sea, Antarctica, Deep Sea Research Part A. Oceanographic Research Papers, 39, 2, 153-168, 1992.

Smith, W. O. and Nelson, D. M.: Importance of ice edge phytoplankton production in the Southern Ocean, BioScience, 36, 4, 251-257, 1986.

Taylor, F., McMinn, A., and Franklin, D.: Distribution of diatoms in surface sediments of Prydz Bay, Antarctica, Marine Micropaleontology, 32,3-4, 209-229, 1997.

Williams, M.: *RV Tangaroa* Voyage Report Tan1302- Mertz Polynya Voyage 1 February to 14 March 2013, *NIWA, Wellington, New Zealand,* 19-33, 80, 2013.

Zielinski, U. and Gersonde, R.: Diatom distribution in Southern Ocean surface sediments (Atlantic sector): Implications for paleoenvironmental reconstructions, Palaeogeography, Palaeoclimatology, Palaeoecology, 129, 3-4, 213-250, 1997.

Williams, G., Aoki, S., Jacobs, S., Rintoul, S., Tamura, T. and Bindoff, N.: Antarctic bottom water from the Adélie and George V Land coast, East Antarctica (140–149 E), Journal of Geophysical Research: Oceans, 115, C4, 2010.

Williams, G., Bindoff, N., Marsland, S. and Rintoul, S.: Formation and export of dense shelf water from the Adélie Depression, East Antarctica, Journal of Geophysical Research: Oceans, 113, C4, 2008.

Wilson, D. J., Bertram, R. A., Needham, E. F., van de Flierdt, T., Welsh, K. J., McKay, R. M., Mazumder, A., Riesselman, C. R., Jimenez-Espejo, F. J. and Escutia, C.: Ice loss from the East Antarctic Ice Sheet during late Pleistocene interglacials, Nature, 561, 7723, 383, 2018.